คุณลักษณะและสมบัติในการเร่งปฏิกิริยาของตัวเร่งปฏิกิริยา Pd/SiO$_2$ ขนาดนาโนเมตร

เตรียมโดยวิธีเฟลมสเปรย์ไพโรไลซิส

นางสาว สิริมา สมบูรณ์ธนกิจ

วิทยานิพนธ์นี้เป็นส่วนหนึ่งของการศึกษาตามหลักสูตรปริญญาวิศวกรรมศาสตรมหาบัณฑิต

สาขาวิชาวิศวกรรมเคมี ภาควิชาวิศวกรรมเคมี

คณะวิศวกรรมศาสตร์ จุฬาลงกรณ์มหาวิทยาลัย

ปีการศึกษา 2550

CHARACTERISTICS AND CATALYTIC PROPERTIES OF NANO-Pd/SiO$_2$
CATALYSTS PREPARED BY FLAME SPRAY PYROLYSIS

Miss Sirima Somboonthanakij

A Thesis Submitted in Partial Fulfillment of the Requirements
for the Degree of Master of Engineering Program in Chemical Engineering
Department of Chemical Engineering
Faculty of Engineering
Chulalongkorn University
Academic Year 2007

Thesis Title	CHARACTERISTICS AND CATALYTIC PROPERTIES OF NANO-Pd/SiO$_2$ CATALYST PREPARED BY FLAME SPRAY PYROLYSIS
By	Miss Sirima Somboonthanakij
Field of study	Chemical Engineering
Thesis Advisor	Assistant Professor Joongjai Panpranot, Ph.D.
Thesis Co-Advisor	Assistant Professor Okorn Mekasuwandamrong, Ph.D.

Accepted by the Faculty of Engineering, Chulalongkorn University in Partial Fulfillment of the Requirements for the Master's Degree
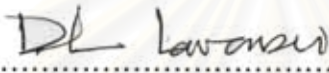
.... Dean of the Faculty of Engineering
(Professor Direk Lavansiri, Ph.D.)
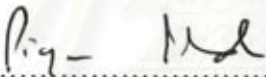
THESIS COMMITTEE

.... Chairman
(Professor Piyasan Praserthdam, Dr.Ing.)
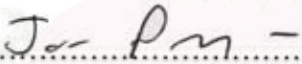
.... Thesis Advisor
(Assistant Professor Joongjai Panpranot, Ph.D.)
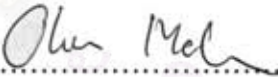
.... Thesis Co-Advisor
(Assistant Professor Okorn Mekasuwandamrong, Ph.D.)

.... Member
(Assistant Professor Bunjerd Jongsomjit, Ph.D.)

.... Member
(Assistant Professor Muenduen Phisalaphong, Ph.D.)

สิริมา สมบูรณ์ธนกิจ: คุณลักษณะและสมบัติในการเร่งปฏิกิริยาของตัวเร่งปฏิกิริยา Pd/SiO$_2$ ขนาดนาโนเมตรที่เตรียมโดยวิธีเฟลมสเปรย์ไพโรไลซิส (CHARACTERISTICS AND CATALYTIC PROPERTIES OF NANO-Pd/SiO$_2$ CATALYST PREPARED BY FLAME SPRAY PYROLYSIS) อ. ที่ปรึกษา: ผศ. ดร. จูงใจ ปั้นประณต, อ. ที่ปรึกษาร่วม: ผศ. ดร. โอกร เมฆาสุวรรณดำรง, 81 หน้า

วิธีเฟลมสเปรย์ไพโรไลซิสถูกใช้สำหรับการสังเคราะห์ตัวเร่งปฏิกิริยา Pd/SiO$_2$ ขนาดนาโน ที่ประกอบด้วยแพลเลเดียม 0.5-10 เปอร์เซ็นต์โดยน้ำหนัก อนุภาคแพลเลเดียมมีการกระจายตัวสูง โดยมีขนาดอนุภาคไม่ใหญ่กว่า 3 นาโนเมตร ถึงแม้ว่ามีปริมาณแพลเลเดียมสูงถึง 10 เปอร์เซ็นต์โดย น้ำหนัก เมื่อทำการเปรียบเทียบกับตัวเร่งปฏิกิริยาที่เตรียมโดยวิธีเคลือบฝังบนตัวรองรับซิลิกาที่ สังเคราะห์โดยวิธีเฟลมสเปรย์ไพโรไลซิสที่มีปริมาณแพลเลเดียมตั้งแต่ 0.5 ถึง 10 เปอร์เซ็นต์โดย น้ำหนัก และตัวเร่งปฏิกิริยาอ้างอิง (แพลเลเดียม 0.5-2 เปอร์เซ็นต์โดยน้ำหนักบนตัวรองรับซิลิกา เชิงพาณิชย์เตรียมโดยวิธีการแลกเปลี่ยนประจุและตัวเร่งปฏิกิริยาลินด์ลาร์ในปฏิกิริยาไฮโดรจิเนชัน แบบเลือกเกิดของ1-เฮปทายภายใต้สภาวะไม่รุนแรงพบว่าตัวเร่งปฏิกิริยาที่เตรียมโดยวิธีเฟลม สเปรย์มีค่า TOF สูงกว่าตัวเร่งปฏิกิริยาที่เตรียมโดยวิธีเคลือบฝังและตัวเร่งปฏิกิริยาอ้างอิง โดยเฉพาะอย่างยิ่งสำหรับตัวเร่งปฏิกิริยาที่มีปริมาณแพลเลเดียมต่ำ ($\leq$ 2 เปอร์เซ็นต์โดยน้ำหนัก) ทั้งนี้คาดว่าสำหรับตัวเร่งปฏิกิริยาที่เตรียมโดยวิธีเฟลมสเปรย์ที่มีปริมาณแพลเลเดียมต่ำอาจมีหมู่ Si-O ปกคลุมแพลเลเดียมขนาดเล็ก และ/หรือ อันตรกิริยาระหว่างแพลเลเดียมและซิลิกาอย่างแข็งแรง เป็นผลให้เกิดการยับยั้งการดูดซับทางเคมีของคาร์บอนมอนนอกไซด์ ทั้งนี้ TOF ของตัวเร่งปฏิกิริยา ที่เตรียมโดยวิธีเฟลมสเปรย์ลดลงจาก 66.2 เป็น 4.3 ต่อวินาที เมื่อมีปริมาณแพลเลเดียมเพิ่มขึ้นจาก 0.5 เป็น 10 เปอร์เซ็นต์โดยน้ำหนัก ในขณะที่ TOF ของตัวเร่งปฏิกิริยาอื่นๆเปลี่ยนแปลงอยู่ในช่วง 3-9 ต่อวินาที อย่างไรก็ตามในทุกตัวเร่งปฏิกิริยา ไม่มีผลต่อการเลือกเกิดของผลิตภัณฑ์1-เฮปทีน

ภาควิชา ....วิศวกรรมเคมี............	ลายมือชื่อนิสิต .....สิริมา.....สมบูรณ์ธนกิจ.....	
สาขาวิชา ....วิศวกรรมเคมี............	ลายมือชื่ออาจารย์ที่ปรึกษา	
ปีการศึกษา ....2550............	ลายมือชื่ออาจารย์ที่ปรึกษาร่วม	

4870522621: MAJOR   CHEMICAL ENGINEERING

KEYWORDS: FLAME SPRAY PYROLYSIS / SILICA SUPPORTED PALLADIUM CATALYST / LIQUID-PHASE HYDROGENATION / 1-HEPTYNE HYDROGENATION

SIRIMA SOMBOONTHANAKIJ : CHARACTERISTICS AND CATALYTIC PROPERTIES OF NANO-Pd/SiO$_2$ CATALYST PREPARED BY FLAME SPRAY PYROLYSIS THISIS ADVISOR : ASST. PROF. JOONGJAI PANPRANOT Ph.D., THESIS CO-ADVISOR : ASST. PROF. OKORN MEKASUWANDUMRONG Ph.D., 81 pp.

Flame spray pyrolysis (FSP) method was used for the synthesis of nano-Pd/SiO$_2$ catalysts containing 0.5 - 10 wt% Pd. Well-dispersed Pd nanoparticles with average Pd particle size not larger than 3 nm were obtained even for the Pd loading as high as 10 wt%. For comparison purposes, the catalysts prepared by conventional impregnation on the flame-made silica with Pd loading 0.5-10 wt% and reference catalysts (0.5-2 wt% Pd loading on commercial SiO$_2$ prepared by ion-exchange method and Lindlar catalyst) were studied. The catalyst activities were tested in liquid-phase semihydrogenation of 1-heptyne under mild conditions. The remarkable high TOF values were noticed for the flame-made catalysts compared to those of the impregnation-made and the reference catalysts especially for those with low Pd loadings ($\leq$ 2 wt%). It is suggested that for the flame-made catalysts with low Pd contents, there was a growth of Si-O groups covering small Pd metals and/or strong Pd-SiO$_2$ interactions resulting in an inhibition of CO chemisorptions. The TOFs of flame-made catalysts decreased from 66.2 to 4.3 s^{-1} with increasing Pd loading from 0.5 to 10 wt% whereas those of the other catalysts were varied between 3-9 s^{-1}. However, in all cases, there was no effect on 1-heptene selectivity.

Department ...Chemical Engineering...... Student's signature ...Sirima.....Somboonthanakij

Field of Study ...Chemical Engineering... Advisor's signature ...Jo- P-u-...

Academic year ....2007.............. Co-advisor's signature ...Olun Meh...

ACKNOWLEDGEMENTS

The author would like to express her greatest gratitude to her advisor, Assistant Professor Joongjai Panpranot, for her help, invaluable suggestions and guidance throughout the entire of this work. She would also like to gratefully acknowledge her co-advisor, Assistant Professor Okorn Mekasuwamdamrong from Department of Chemical Engineering, Silpakorn University, for a number of suggestions and kindness understanding.

The author wishes to express her thanks to Professor Piyasan Praserthdam who has been the chairman of the committee for this thesis, and Associate Professor Bunjerd Jongsomjit and Associate Professor Muenduen Phisalaphong, who have been her committee members.

The author would like to thank all my friends and all members of the Center of Excellent on Catalysis & Catalytic Reaction Engineering (Petrochemical Engineering Research Laboratory), Department of Chemical Engineering, Chulalongkorn University for their assistance and friendly encouragement.

Moreover, the author would like to thank the Thailand Research Fund (TRF), as well as the Graduate School of Chulalongkorn University (Research grant for 90th Anniversary of Chulalokorn University) for their Financial Support. Finally, she would like to dedicate the achievement of this work to her dearest parents. Their unyielding support and unconditional love have always been in her mind.

CONTENTS

LIST OF TABLES

LIST OF FIGURES

FIGURE **Page**

FIGURE   **Page**

FIGURE   **Page**

CHAPTER I

INTRODUCTION

1.1. Rationale

The selective alkyne hydrogenation is the important reaction for the preparation of fine chemicals and biologically activity compounds [1]. The main objective in alkyne semihydrogenation is to achieve the highest alkene selectivity possible. In the field of fine chemical synthesis, palladium is one of the most versatile and most widely applied catalytic metals [2] and selective hydrogenation [3].

Pd is normally used as a supported heterogeneous catalyst. The advances of the reaction in heterogeneous condition are the rapid removal of the hydrogenated products, easy recovery, and catalytic recycling [4, 5]. The previous studies of Pd selectivity is attributed to stronger chemisorption of the alkyne species on the active center than that of the alkane, which is related to the high electron density and the restricted rotation of the $C \equiv C$ bond [1]. A commonly used catalyst for the semihydrogenation of alkynes is a commercial Lindlar catalyst, 5 wt% Pd on calcium carbonate, modified by the addition of lead to improve selectivity [6].

As the reported by several authors, high activity and selectivity may be obtained over other catalyst. Systems in which modifiers are not necessary such as Pd/montmorillonite [7], Pd/hydrotalcite [1], Pd-Cu/SiO_2 [2], Pd/activated carbon, Pd/TiO_2, and Pd/ -Al_2O_3 [8], supported Pd complex and Lindlar catalyst [9]. These catalyst systems, however, may require several steps during preparation such as calcination and high temperature reduction pretreatment in order to obtain high catalytically active components.

Flame aerosol synthesis has been used to produce various nanoparticles such as ceramic, metal and composite powders because it provides good control of particle size, particle crystal structure and this method also can produce highly pure particles continuously without further subsequent process, for example, drying, calcinations, and milling in the wet chemical processes. The sizes of flame-made particles range

from a few to several hundred nanometers in diameter depending on process conditions [2, 10]. Flame aerosol synthesis is used on a large scale today to produce carbon black, fumed silica, and titania pigments. In general flame synthesis is a fast, cost-effective, and versatile process for the production of a wide variety of different nanoparticles and especially flame spray pyrolysis. In this process a flame is used to drive chemical reactions of precursor compounds, resulting in the formation of clusters, which grow to nanometer-sized products by coagulation and sintering [2, 11].

The important problem in catalytic liquid phase hydrogenation is the activity and selectivity decay due to catalyst deactivation. The main causes of catalyst deactivation in liquid phase hydrogenation are

1. Sintering of metal particles and coalescence
2. Leaching of active phases and supports
3. Poisoning of strongly adsorbed molecules

Because the cost of these noble metal catalysts used in theses reactions are very high, this problem must be concerned [12].

1.2. Objective

The objective of this research has been to study the characteristics and catalytic properties of silica-supported palladium catalysts prepared by flame spray pyrolysis in liquid-phase selective hydrogenation reaction of alkynes.

1.3. Research Scopes

Part I

1. Preparation of silica-supported palladium (Pd/SiO_2) with 0.5 – 10 wt% Pd loadings and silica supports by flame spray pyrolysis method (FSP).
2. Loading 0.5 – 10 wt% Pd on the flame-made silica support using incipient wetness impregnation method.
3. Characterization of silica-supported palladium catalysts using several techniques such as X-ray diffraction (XRD), transmission electron microscopy (TEM), N_2 physisorption, CO-pulse chemisorption, and X-ray Photoelectron Spectroscopy (XPS).
4. Reaction study of silica-supported palladium catalysts in liquid-phase hydrogenation of an alkyne using stirring batch reactor (stainless steel autoclave 50 ml).
5. Study of catalyst deactivation after performing liquid-phase hydrogenation.

Part II

1. Reaction study of other Pd/SiO_2 and commercial catalysts (0.5 - 2 wt% Pd prepared by ion-exchange method on commercial silica and Lindlar catalyst) in liquid-phase hydrogention of an alkyne.

CHAPTER II

THEORY

2.1 Flame Spray Pyrolysis (FSP)

Flame synthesis is a relatively new method for the one-step production of supported noble metal catalysts and catalysts in general. Flame aerosol synthesis is a cost-effective and versatile process for the controlled production of nanoparticles. In flame reactors, the energy of a flame is used to drive chemical reactions of precursor compounds that result in the formation of clusters which further grow by coagulation and sintering in the hot flame environment to nanometer-sized product particles [2, 11].
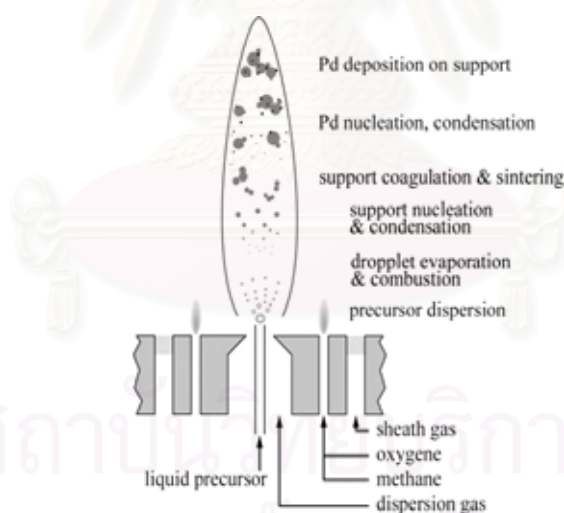
Figure 2.1   Skecth of the flame spray pyrolysis unit [2]

There are two primary types of the flame aerosol process for the synthesis of those nanoparticles. One is a flame assisted vapor-to-particle conversion process that is called as flame vapor synthesis (FVS). The other is a flame assisted liquid droplet-to-particle conversion process called as flame spray pyrolysis (FSP). The FVS process

is the best choice for the synthesis of solid nanoparticles of single-component and binary systems such as metals, semiconductors, simple oxide, nitrides, etc. However, the FVS process requires the use of volatile precursors. High production rate is possible when highly volatile precursors are available, and because the vapor phase precursors can be purified more easily than solid or liquid precursors, the FVS process allows the generation of materials with ultrahigh purities. Unfortunately, a disadvantage of the FVS process is that the synthesis of high-purity volatile precursors is complicated and expensive.

In general, the FVS is more complex to design and operate than the FSP because the FVS requires a gas-handling subsystem for the controlled introduction of vapor phase reactants. In contrast, the FSP systems require only an atomizer. The FSP has the major advantages that can handle materials containing a large number of elements and that aqueous solution of precursors can be used to produce multi-components oxide nanoparticles [10].

In conventional spray pyrolysis, the solution is atomized into a hot wall reactor where the aerosol droplets undergo evaporation and solute concentration within the droplet, drying, thermolysis of the precipitate particle at higher temperature to form a microporous particle, and, eventually a dense one by sintering. The advantages of FSP include the ability to dissolve the precursor directly in the fuel, simplicity of introduction of the precursor into the hot reaction zone (e.g. a flame), and flexibility in using the high-velocity spray jet for rapid quenching of aerosol formation [13].

When producing nano-catalyst using a high temperature flame, the particle collection technique has to be chosen. One solution is to collect the material directly on the substrate either inside the flame or very close to it. The variety of operational details includes several physical parameters such as e.g. particle size of the material. When nanosized particles are deposited on the substrate, it is assumed that coarsening of the material may take place, including partial sintering, neck formation and even full coalescence of the particles, especially if the temperature is sufficiently high.
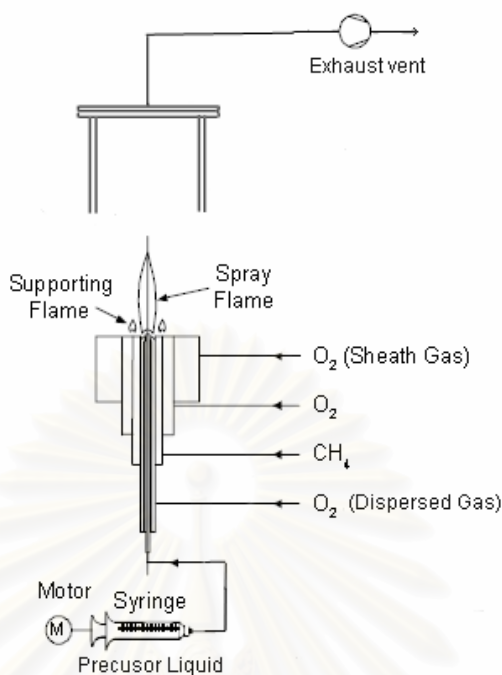
Figure 2.2   Experimental set-up for Pd/SiO$_2$ catalysts synthesis by flame spray pyrolysis

2.2 Liquid-Phase Hydrogenation

Liquid phase hydrogenation covers a huge range of processes, from the hydrogenation of vegetable oils and various sweeteners to hydrocarbons within the petrochemical industry. Even though classified as hydrogenation, all are very different processes, with their own characteristic process solutions. They possess some common features nevertheless, such as mass transfer and reliance on a catalyst. Indeed there are more hydrogenation catalysts available commercially than any other type, and for good reason, because hydrogenation is one of the most useful, versatile and environmentally acceptable reaction routes for organic synthesis. Typically the catalyst is powdered and slurried with reactant; a solvent is usually present to influence product selectivity and to adsorb the reaction heat liberated by the reaction. Since most hydrogenations are highly exothermic, careful temperature control is required to achieve the desired selectivity and to prevent temperature runaway.

2.3 Hydrogenation of Alkynes

Addition of hydrogen to a carbon-carbon double bond or triple bond is called hydrogenation. The overall effect of such an addition is the reductive removal of the double bond functional group. Regioselectivity is not an issue, since the same group (a hydrogen atom) is bonded to each of the double bond carbons. The simplest source of two hydrogen atoms is molecular hydrogen (H_2), but mixing alkenes or alkynes with hydrogen does not result in any discernable reaction. Although the overall hydrogenation reaction is exothermic, a high activation energy prevents it from taking place under normal conditions. This restriction may be circumvented by the use of a catalyst, as shown in the following diagram.
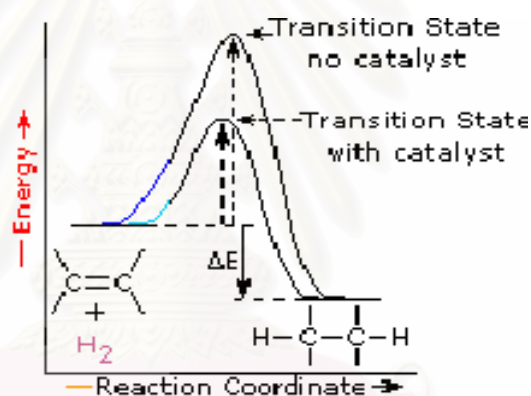
Figure 2.3   Free-energy diagrams for the hydrogenation of an alkene in the presence of a catalyst and the hypothetical reaction in the absence of a catalyst

As shown in the energy diagram, the hydrogenation of alkenes is exothermic, and heat is released corresponding to the ΔE in the diagram. This heat of reaction can be used to evaluate the thermodynamic stability of alkenes having different numbers of alkyl substituent on the double bond.

Catalysts are substances that change the rate (velocity) of a chemical reaction without being consumed or appearing as part of the product. Catalysts act by lowering the activation energy of reactions, but they do not change the relative potential energy of the reactants and products. Finely divided metals, such as platinum, palladium and

nickel, are among the most widely used hydrogenation catalysts. Catalytic hydrogenation takes place in at least two stages, as depicted in the diagram.

H-H

Step 1:

Hydrogen gets absorbed onto the metal surface.

Step 2:

Alkyne approaches the H atoms absorbed on the metal surface.

Step 3:

C≡C reacts with the H atoms on the surface forming the two new C-H s bonds generating the alkene, which is more weakly adsorbed, leaves the catalyst surface.
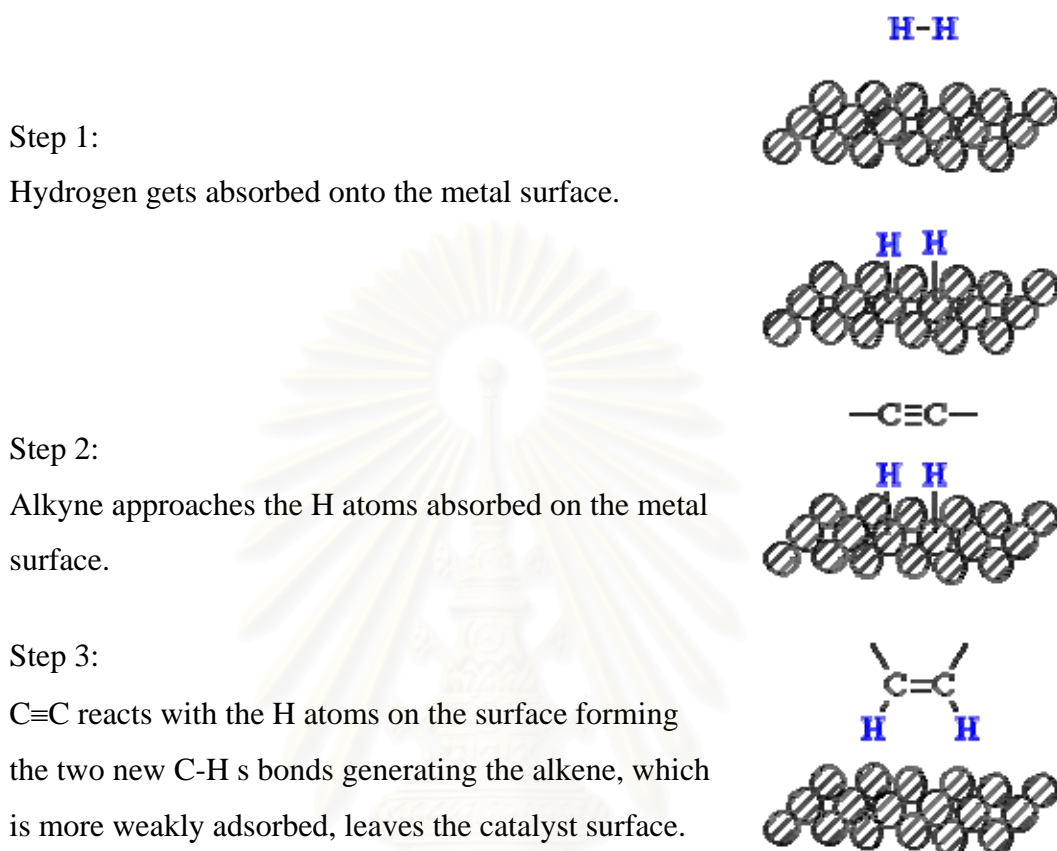
Figure 2.4   Show mechanism of hydrogenation of alkyne

CHAPTER III

LITERATURE REVIEWS

3.1 Flame Spray Pyrolysis (FSP)

L. Madler et al. [13] achieved for synthesis of nanostructured silica particles with closely controlled specific surface area by FSP. For a liquid mixture of HMDSO/ethanol with a molar ratio of 0.1 resulting in a SiO_2 production rate of 9 g/h, the specific surface area of the product ranged from 391 to 70 m^2/g corresponding to an equivalent particle diameter of 7–40 nm. At low oxidant flow rates, the specific surface area increases with increasing oxidant flow rate as the spray flame length is reduced leading to shorter residence time allowing less time for particle growth. Using oxygen as oxidant the droplets burn much faster than with air, thus, product particles experience longer residence times at higher temperature and, as a result, they have lower specific surface area compared to those made using air as confirmed by in situ flame spray temperature measurements. The product specific surface area exhibited a maximum and decreases for higher oxidant flow rates. At high flow rates the flame height is reduced substantially as fuel and precursor are oxidized faster in a smaller unit volume accelerating, thus, precursor release at higher temperatures leading to high sintering rates and therefore smaller specific surface area of the product.

R. Mueller et al. [14] investigated continuous FSP synthesis of nanostructured silica particles with closely controlled characteristics at high production rates (up to 1.1 kg/d) in a pilot plant using baghouse filters. The infuence of silica powder production rate, precursor concentration and oxidant dispersion gas flow rate was investigated on the product primary particle diameter, morphology and carbon content using HMDSO in EtOH at 1.26 and 3:0 M as well as pure HMDSO (4:7 M). The average product primary particle size was controlled from 10 to 75 nm independent of precursor concentration confirming that particle formation can take place during FSP

in the gas phase following rapid evaporation of precursor droplets. The control of primary particle size using FSP is similar to that by the well-established vapor-fed aerosol reactors through the oxidant or precursor delivery rates. Limited variation of the product particle size was obtained when using air instead O_2 as dispersion gas (at constant pressure drop across the nozzle) or by providing additional sheath O_2 gas.

R. Stobel et al. [2] studied flame spray synthesis of Pd/Al_2O_3 catalysts and their behavior in enantioselective hydrogenation. They prepared 1 - 7.5 wt% Pd using flame spray pyrolysis (FSP). The result showed that palladium dispersion depended on the metal loading and decreased for higher amounts of Pd and then tested for the enantioselective hydrogenation of 4-methoxy-6-methyl-2-pyrone. Rate and enantioselectivity decreased with higher Pd dispersion. However, hydrogen pretreatment of the flame-made catalysts at $500^{o}C$ improved rate and enantioselectivity strongly. Enantiomeric excess in the formation of (*R*)-4-methoxy-6-methyl-5,6-dihydro-2-pyrone reached 80% for flame-made catalysts after pretreatment in hydrogen. Hydrogen pretreatment temperatures above $600^{o}C$ led to sintering of the Pd particles and drastic loss in activity and enantioselectivity.

H. D. Jang et al. [10] studied synthesis of SiO_2 nanoparticles from sprayed droplets of tetraethylorthosilicate by the flame spray pyrolysis. TEOS concentration, maximum flame temperature, and residence time of reactants in the flame were chosen as key experimental variables for the control of the particle morphology, and average particle diameter. Larger particles were produced with decrease of the maximum flame temperature by controlling of hydrogen flow rate and oxygen in the burner. Average particle diameter increased with the increase of residence time by controlling the carrier gas flow rate.

Up till now a variety of products have been synthesized by FSP as shown in Table 3.1.

Table 3.1   Some products obtained from flame spray pyrolysis method.

Product	Reference
Zinc oxide	Marshall, Telford, and Wood [15]
Alumina	Sokolowski, Sokolowska, Michalski, and Gokieli [16]; Tok, Boey, and Zhao [17]
Magnesium-aluminate	Bickmore, Walder, Treadwell, and Laine [18]
γ-ferric oxide	Grimm, Schultz, Barth, and Muller [19]
Titania/silica	Stark, Pratsinis, and Baiker [20]
Oxide-supportd gold-silver	Hannemann, Grunwaldt, Krumeich, Kappen, amd Baiker [21]

3.2 Supported Pd Catalysts in Liquid-Phase Selective Hydrogenation

S. D. Jackson and L. A. Shaw [22] studied the hydrogenation of phenyl acetylene and styrene over a palladium/carbon catalyst. The kinetics of the reactions were investigated and activation energies of 26 ± 2 kJ/mol and 41 ± 8 kJ/mol were obtained for phenyl acetylene hydrogenation and styrene hydrogenation, respectively. Both reactions were found to be zero order concerning the alkyne or alkene. However the order in phenyl acetylene changed from zero order to first order at approximately 60% conversion. This change was due to the effect of styrene co-adsorption and not the concentration of phenyl acetylene. Competitive hydrogenation between the alkene and alkyne resulted in a dramatically reduced rate of hydrogenation for both species. This reduced rate was explained by a reduction in the amount of surface hydrogen as well as the altered bonding of the phenyl acetylene.

A. Molnar et al. [23] reviewed the selective hydrogenation of hydrocarbons with multiple unsaturation (dienes and alkynes) over heterogeneous palladium catalysts. Factors such as metal dispersion, carbon deposits, and the use of promoters and additives controlling catalytic activities and chemo-, regio- and stereo-selectivity are discussed. A detailed treatment of the status of the selective removal of hydrocarbon impurities with multiple unsaturation from industrial feedstocks is also given.

P.C. L'Argentiere et al. [24] studied supporting on γ-Al$_2$O$_3$ a palladium complex with chloride and tridecylamine as ligands. It is more active and selective for the 1-heptyne hydrogenation to 1-heptene than the classic Lindlar's catalyst. At the same operational conditions, the supported palladium complex is also more active and selective than the same complex unsupported. The hydrogen pressure and the operational temperature showed to play an important role in the catalytic behavior of the catalysts under study. As determined by FTIR and X-ray photoelectron spectroscopy (XPS), the active species is the complex itself, which is stable under the reaction conditions. The obtained XPS results show that the palladium complex, supported or not, is tetra-coordinated, suggesting that its formula is [PdCl$_2$(NH$_2$(CH$_2$)$_{12}$CH$_3$)$_2$]. The highest activity and selectivity of the palladium supported complex can be attributed, at least partially, to electronic and geometrical effects.

A. Mastalir et al. [1] prepared Pd nanoparticles incorporated in a hydrotalcite (HT) host via anion exchange between a dilute suspension of HT–nitrate and a Pd hydrosol stabilized by the anionic surfactant sodium dodecyl sulfate. Samples of two of the resulting Pd organoclays, Pd–HT1 and Pd–HT2, with metal contents of 0.1 and 0.42%, respectively, were subjected to further investigations. Characterization via ICP-AES, XRD, and TEM measurements indicated the deposition of fairly monodispersed Pd particles, predominantly on the external surface of the HT layers. The Pd–HT samples proved to be efficient catalysts for the liquid-phase semihydrogenations of both terminal and internal alkynes under mild conditions. For the transformation of phenylacetylene to styrene, a bond selectivity of 100% was obtained, and the *cis* stereoselectivities for the hydrogenations of the internal alkynes 4-octyne and 1-phenyl-1-pentyne reasonably approached 100%. The catalytic activity of Pd–HT increased with the Pd dispersion, whereas the alkene selectivity remained essentially unaffected.

M.G. Mosulino et al. [25] investigated hydrogenation of 2-butyne-1,4-diol over palladium supported catalysts. It was found that, besides butane-1,4-diol, side products such as *cis*- and *trans*-2-butene-1,4-diol, 2-hydroxytetrahydrofuran, *cis*- and

trans-crotyl alcohol and *n*-butanol were also formed. The influence of proton, nature of solvent and carbon support on activity and products distribution has been studied in the hydrogenation of *cis*-2-butene-1,4-diol. The use of water as solvent shows a better activity and selectivity to butane-1,4-diol and suppresses the hydrogenolysis reaction more than other solvents used. A higher activity and selectivity to isomerisation products were obtained on the palladium catalysts supported on acid modified carbon.

T.A. Nijhuis et al. [3] prepared silica-supported palladium catalysts for the selective liquid-phase hydrogenation of alkynes to alkenes. As a model reaction the hydrogenation of 3-methyl-1-pentyn-3-ol was chosen. The kinetics of this reaction were investigated. Different approaches were used to obtain an optimal catalyst system. The selectivity of the palladium catalysts was successfully improved by modifying the catalyst with copper and the effect of this modification on the reaction mechanism was studied. The addition of quinoline as a reaction modifier to the system was investigated as a manner to improve selectivity. Monolith supported catalysts were prepared to obtain a more convenient reactor configuration.

A. Mastalir et al. [26] prepared 0.15% Pd loading of organophilic Pd-M samples by cation exchange in a micellar system. The Pd particle size was controlled by varying the precursor and surfactant concentrations. The samples Pd-M1, Pd-M2 and Pd-M3, with mean particle diameters of 1.5, 3.0 and 6.2 nm, respectively, were subjected to further investigations. Increase of the particle diameter was found to broaden the size distribution. The samples were tested as catalysts for the liquid-phase semihydrogenations of phenylacetylene and 4-octyne under mild conditions. The catalytic activity was demonstrated to increase with the Pd dispersion, unlike the selectivity of styrene formation, which remained unchanged. The most efficient catalyst at S:Pd = 2000 was Pd-M1, the sample with the highest dispersion. The catalytic activities of Pd-M2 and Pd-M3 could be substantially improved by decreasing the S:Pd ratio to 800. For the semihydrogenation of 4-octyne, the Pd-M samples proved to be moderately active, but highly stereoselective catalysts. Similarly to the reaction of phenylacetylene, when the particle diameter exceeded 4 nm, a significant loss in the catalytic activity was experienced as the reaction progressed.

A. Papp et al. [27] synthesized Pd-MCM-41 samples with different Pd contents by using $PdCl_2$, tetraethyl orthosilicate (TEOS) and the cationic surfactant cetyltrimethylammonium bromide (CTAB). The representative samples Pd-MCM(1.39) and Pd-MCM(5.85) had Pd contents 1.39 and 5.85%, respectively. Although the formation of the Pd particles was found to decrease the crystalline character of the host material, the structure of the MCM-41 framework was retained for both samples. Both samples proved to be active and selective catalysts for the liquid-phase semihydrogenations of phenylacetylene, 3-butyn-1-ol, 4-octyne and 1-phenyl-1-butyne. The initial activity of Pd-MCM(1.39) surpassed that of Pd-MCM(5.85) for each reaction, indicating that the catalytic activity was dependent on the Pd crystallite size. For the semihydrogenation of 4-octyne, Pd-MCM(1.39) proved to be an extremely efficient catalyst. The catalytic activities of the Pd-MCMs were considerably higher than those of silica-supported Pd catalysts.

P. A. Robles-Dutenhefner et al. [28] prepared sol-gel palladium slilica composites for the selective hydrogenation of myrcene. Catalysts treated at $1100^{o}C$ give monohydrogenated products with excellent combined selectivity of 90–95% at almost complete conversion of the substrate. The selective monohydrogenation of myrcene could be useful to produce a mixture of diolefins of different reactivity, which could be further transformed to oxygenated derivatives with selectivities better than myrcene itself.

3.3 Deactivation of Supported Pd Catalysts in Liquid-Phase Reaction

P. Albers et al. [29] summarized some of the major causes for deactivation and premature degradation of palladium catalysts. These include particle growth for various reasons, coke deposition and coke transformation, the influence of the support material on long term stability and modifications at the palladium surface itself such as valency changes or the formation of simple but stable molecular surface species.Observations on different deactivation processes on Pd/SiO_2 catalysts occuring under industrial conditions are compiled. It was tried to roughly differentiate between different degrees of coking and coke transformation in mainly thermally or purely catalytically driven catalyst coking on the one hand and of moderate or enhanced corrosion phenomena or changes of the properties of the palladium itself on the other.

M. Besson et al. [30] gave a general survey of the factors contributing to the deactivation of metal catalysts employed in liquid phase reactions for the synthesis of fine or intermediate chemicals. The main causes of catalyst deactivation are particle sintering, metal and support leaching, deposition of inactive metal layers or polymeric species, and poisoning by strongly adsorbed species. Weakly adsorbed species, poisons at low surface coverage and solvents, may act as selectivity promoters or modifiers. Three examples of long term stability studies carried out in trickle-bed reactor (glucose to sorbitol hydrogenation on Ru/C catalysts, hydroxypropanal to 1,3-propanediol hydrogenation on Ru/TiO$_2$ catalysts, and wet air oxidation of paper pulp effluents on Ru/TiO$_2$) are discussed.

3.4 Comments on the Previous Studies

From literature reviews, catalysts are typically prepared by wet-phase chemistry followed by filtration, drying, and calcinations to remove undesired residuals and homogenize the surface. Alternatively, flame technology may provide a direct, continuous process with few waste and by-product generation. Depending on the synthesis condition, specific surface area and size of metal on the catalysts can be controlled. Moreover high-temperature preparation favors the distribution of an active component on the surface of the catalyst and often leads to narrow site distribution. Pd is the one of the most useful catalysts used in liquid-phase hydrogenation reaction. Furthermore types of solvent and support show the important roles in catalytic activity and catalyst deactivation. In the recent years, supercritical carbon dioxide has been increasingly used as an environmentally friendly reaction medium in place of toxic and hazardous organic solvents. Catalyst deactivation such as leaching is the problem that usually occurs in these reactions. However, the properties of flame-made palladium/silica catalysts in catalytic liquid-phase hydrogenation and deactivation have not been well studied so far. Thus, it is the aims of this study to synthesize silica-supported palladium by flame spray pyrolysis in liquid-phase hydrogenation.

CHAPTER IV

EXPERIMENTAL

4.1 Catalyst Preparation

Catalyst support used in this study is flame-derived silica and is denoted as silica-FSP.

4.1.1 Materials

The chemical used in this study are specified as follows in Table 4.1.

Table 4.1   Chemicals used in the synthesis of flame-made catalyst

Chemical	Supplier
Palladium acetylacetonate ($Pd(acac)_2$)	Aldrich
Tetraethylorthosilicate (TEOS)	Aldrich
Xylene (99.8 vol.%)	MERCK
Acetonitrile (99.5 vol.%)	Fluka

4.1.2   Synthesis of Flame-Made Catalyst and Silica-Supported

The synthesis of silica of silica-supported palladium nanoparticles was carried out by flame spray pyrolysis. Palladium acetylacetonate and tetraethylorthosilicate were chosen as raw materials for preparation of a liquid-phase precursor. Precursors were prepared by dissolving in xylene/acetonitrile mixtures (70/30 vol%). The total concentration was always 0.5 M. The palladium concentration was ranged between 0 and 10wt%. During particle synthesis, 5 ml/min of liquid precursor were fed to the flame by a syringe pump and dispersed with 5 l/min oxygen forming fine spray

droplets. The pressure drop at the capillary tip was maintained at 1.5 bar by adjusting the orifice gap area at the nozzle. The spray was ignited by supporting flamelets fed with oxygen (3 l/min) and methane (1.5 l/min) which are positioned in a ring around the nozzle outlet. A sintered metal plate ring (8 mm wide, starting at a radius of 8 mm) provided additional 25 l/min of oxygen as sheath for the supporting flame. The product particles were collected on a glass fiber filter (Whatman GF/A, 15 cm in diameter) with the aid of a vacuum pump.

Silica-supported was prepared by the same condition as silica-supported palladium.

4.1.3   Palladium Loading

In this experiment, incipient wetness impregnation was used for loading palladium into flame-derived silica. Palladium acetylacetonate was used as precursor.

The certain amount of palladium precursor (between 0 to 10wt% loading) was introduced into the acetonotrile which its volume equals to pore volume of catalyst. The silica support was impregnated with a palladium solution. The palladium solution was dropped slowly to the silica support, then dried overnight in the oven at 100°C and calcined in air at 450°C for 3 h.

4.2 The Reaction Study in Liquid-Phase Hydrogenation

The liquid-phase hydrogenation was used to study the properties of these prepared catalysts. An alkyne such as 1-heptyne was used as reactant under an organic solvent as reaction medium.

4.2.1   Chemicals and Reagents

The chemicals and reagents used in the reactions are shown in Table 4.2.

Table 4.2   The chemicals and reagents used in the reaction

The chemicals and reagents	Supplier
High purity grade Hydrogen (99.99 vol.%)	Thai Industrial Gases Limited
1-heptyne	Aldrich
1-heptene	TRADE TCI MARK
n-heptane	Wako
Toluene	Fluka

4.2.2   Instrument and Apparatus

The main instruments and apparatus are explained as follow:

The autoclave reactor

The 50 ml stainless steel autoclave was used as reactor. Hot plate stirrer with magnetic bar was used to heat up the reactant and to ensure that the reactant and the catalyst were well mixed.

Gas chromatography

A gas chromatography equipped with flame ionization detector (FID) with GS-alumina capillary column was used to analyze the feed and product.

Table 4.3   Operating condition for gas chromatograph

Gas Chromatograph	Shimadzu GC-14A
Detector	FID
Packed column	GS-alumina (length =30 m, I.D. =0.53 mm)
Carrier gas	Helium (99.99 vol.%)
Make-up gas	Nitrogen (99.99 vol.%)
Column temperature	200°C
Injector Temperature	250°C
Detector Temperature	280°C

4.2.3   Liquid-Phase Hydrogenation Procedure

The reaction study section is liquid-phase hydrogenation of 1-heptyne in toluene and divided into three parts. The first part used flame-made catalysts and catalysts in the second part are come from incipient wetness impregnation on flame-made support. Finally, reference catalysts are used in the same reaction.

4.2.3.1   1-heptyne hydrogenation of FSP-catalysts

0.2 ml of 1-heptyne, 9.8 ml of toluene and 20 mg of catalyst were introduced into the autoclave reactor. The reaction was carried out under hydrogen atmosphere at 1 bar and $30^{o}C$ for 5 min. After the reaction, the vent valve was slowly opened to prevent the loss of product. Then the product mixture was analyzed by gas chromatography with flame ionization detector (FID).

4.2.3.2   1-heptyne hydrogenation of impregnated-FSP-catalysts

This procedure is consisted two steps.

1. Reduction step

Approximately 20 mg of supported palladium catalyst was placed into the glass tube. Then the catalyst was reduced by hydrogen gas at the volumetric flow rate of 50 ml/min at room temperature for 2 h.

2. Reaction step

This step was the same as the procedure of FSP-catalysts hydrogenation.

4.2.3.3   1-heptyne hydrogenation of reference catalysts

There are many catalysts; Pd with Pd loading 0.5 – 2wt% prepared by ion-exchange technique on commercial silica [31] and Lindlar catalysts (N.E. Chemcat).

Lindlar catalysts was required only the reaction step that the same as the procedure of FSP-catalysts hydrogenation. For Pd/SiO$_2$-com catalysts, they were consisted two steps as same as impregnated-FSP-catalysts.

4.3 Catalyst Characterization

The fresh and spent catalyst were characterized by several techniques such as

4.3.1 N$_2$ Physisorption

The surface area of solid, average pore size diameters and pore size distribution were determined by physisorption of nitrogen (N$_2$) using Micromeritics ASAP 2020 (surface area and porosity analyzer).

4.3.2 X-ray Diffraction (XRD)

The bulk crystal structure and chemical phase composition were determined by diffraction of an X-ray beam as a function of the angle of the incident beam. The XRD spectrum of the catalyst was measured by using a SIEMENS D500 X-ray diffractometer and Cu K$_\alpha$ radiation. The crystallite size was calculated from Scherrer's equation.

4.3.3 Transmission Electron Microscopy (TEM) with Diffraction Mode

Catalyst crystallite size and the diffraction pattern of silica support were observed using JEOL-JEM 200CX transmission electron microscope operated at 100kV at National Metal and Materials Technology Center.

4.3.4 CO-Pulse Chemisorption

The active sites and the relative percentages dispersion of palladium catalyst are determined by CO-pulse chemisorption technique using Micromeritics ChemiSorb 2750 (pulse chemisorption system)

4.3.5 X-ray Photoelectron Spectroscopy (XPS)

The XPS spectra, the binding energy and the composition on the surface layer of the catalysts were determined by using a Kratos Amicus X-ray photoelectron spectroscopy. The analyses were carried out with these following conditions: Mg Kα X-ray source at current of 20 mA and 12kV, 0.1 eV/step of resolution, and pass energy 75 eV, and the operating pressure was approximately 1×10^{-6} Pa.

CHAPTER V

RESULTS AND DISCUSSION

Supported noble metal catalysts are widely used in hydrogenation reactions. The flame-made and impregnated catalysts with Pd loading 0.5-10 wt% and the reference catalysts were used in this study. Reference catalysts were Pd/SiO$_2$-com (SiO$_2$ commercial from Stream Chemicals: BET surface area 243 m^2/g, pore volume 1.060 cm^3/g, and pore diameter 17.40 nm) with Pd loading 0.5 – 2 wt% prepared by ion-exchange technique [31] and Lindlar catalysts (N.E. Chemcat). This chapter is divided into three parts: 1) characterization of the catalysts, 2) selective hydrogenation study, and 3) catalyst deactivation.

In the first part, the catalysts were characterized by several techniques such as XRD, TEM, N$_2$ physisorption, AAS, CO-pulse chemisorption, and XPS. The second part is the study of selective 1-heptyne hydrogenation. The reaction was carried out at 30°C and 1 bar of H$_2$ pressure. Finally catalyst deactivations of the flame-made and impregnated catalysts due to metal sintering and metal leaching were also investigated using TEM and AAS techniques.

5.1 Characterization of the Catalysts

5.1.1   X-ray Diffraction (XRD)

The XRD patterns of flame-made Pd/SiO$_2$ catalysts with Pd loading 0 - 10 wt% were carried out at the diffraction angle (2θ) between 10° and 80°, the results are shown in Figure 5.1. All the samples exhibited XRD characteristic peak of amorphous SiO$_2$ (22°2θ) The XRD peaks for Pd^0 metal were observed only for 10 wt% Pd/SiO$_2$. The major peak was shown at 40.1^{o}2θ. It is suggested that palladium particles were finely dispersed and their average particle sizes were smaller than XRD detectable

limit with low Pd loading. Palladium particles in the flame-made catalysts were Pd^0 metals therefore the calcination/reduction step is unnecessary.

Figure 5.2 shows the XRD patterns of all Pd/SiO_2–FSP-im catalysts with Pd loading between 0 to 10 wt%. Impregnated catalysts for all Pd loadings exhibited XRD characteristic peaks the amorphous silica ($22^o 2\theta$) and the main peak of PdO phase at $33^o 2\theta$. The catalysts after reduction in H_2 at 30^oC for 2 h were analyzed by XRD and are shown in Figure 5.3. Pd^0 metal peaks were only apparent for Pd/SiO_2–FSP-im with Pd loading 5 and 10 wt%, suggesting that Pd was probably highly dispersed or its average particle size was smaller than XRD detectable limit.
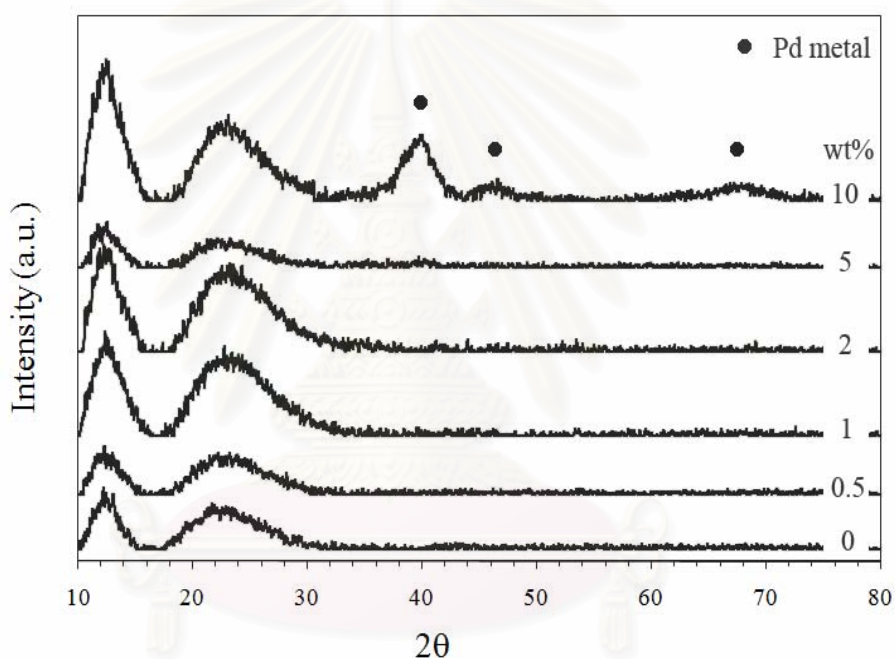
Figure 5.1   XRD patterns of flame-made catalyst with Pd loading between 0 and 10 wt%
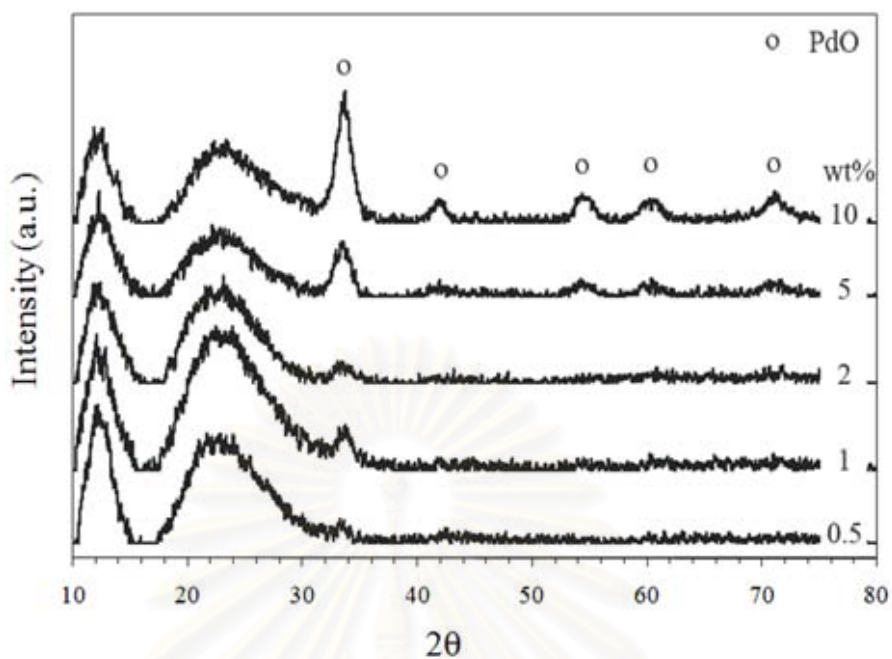
Figure 5.2   XRD patterns of all impregnated Pd/SiO₂ catalyst with Pd loading 0.5-10 wt% without reduction
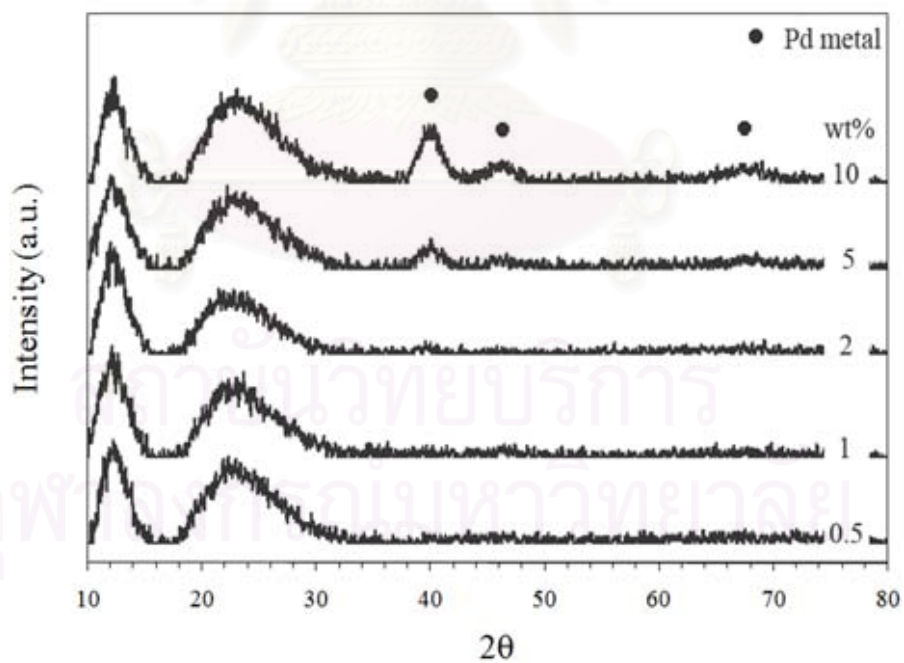
Figure 5.3   XRD patterns of all impregnated Pd/SiO₂ catalyst with Pd loading 0.5-10 wt% after reduction in H₂ at 30°C for 2 h

5.1.2 Transmission Electron Microscopy (TEM)

TEM micrographs were taken for the flame-made SiO_2 and the Pd/SiO_2 catalysts with different Pd contents and are shown in Figure 5.4 to Figure 5.9, respectively. The Pd clusters were found to be in spherical shape with average diameter of 0.5-3 nm with narrow distribution. These Pd particles were confined to the surface of SiO_2 particles. In general, higher palladium loading achieved by increasing Pd content leads to larger metal particles and lower Pd dispersions. The TEM images were similar to the Pd/Al_2O_3, Pt/Al_2O_3, and Pt/TiO_2 prepared via flame process [32, 33, 34]. However, it is surprising that for Pt/SiO_2 prepared by FSP under similar conditions using platinum acetylacetonate as Pt precursor, some very large Pt particles (> 100 nm) were obtained due to incomplete evaporation [35]. This was not the case for the flame-derived Pd/SiO_2 in which only small Pd particles were observed. The average clusters sizes of palladium increased from 0.5 nm to 3 nm as Pd loading increasing from 0.5 to 2 wt% and remained at 3 nm even after increasing of Pd loading to 10 wt%.

TEM with diffraction mode was shown in Figure 5.4 (b). It is used to determine the crystallographic structure of the silica support. It is revealed that the silica-FSP is semi-polycrystalline.

Figure 5.10 to Figure 5.14 show the TEM micrographs of impregnated Pd on flame-made silica with Pd loading 0.5-10 wt%. The Pd clusters were found in spherical shape with 0.4 – 5.3 nm.
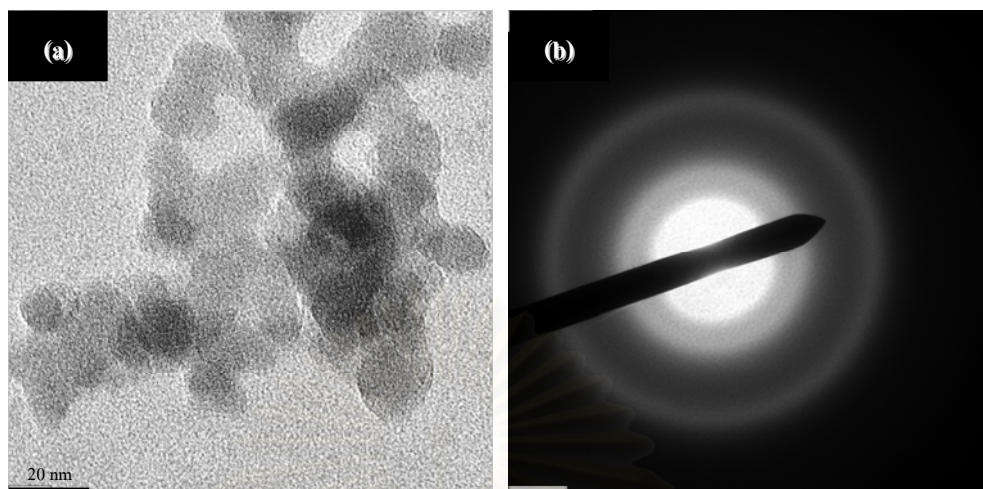
Figure 5.4   SiO$_2$-FSP TEM micrographs (a) and selected area electron

diffraction (b)
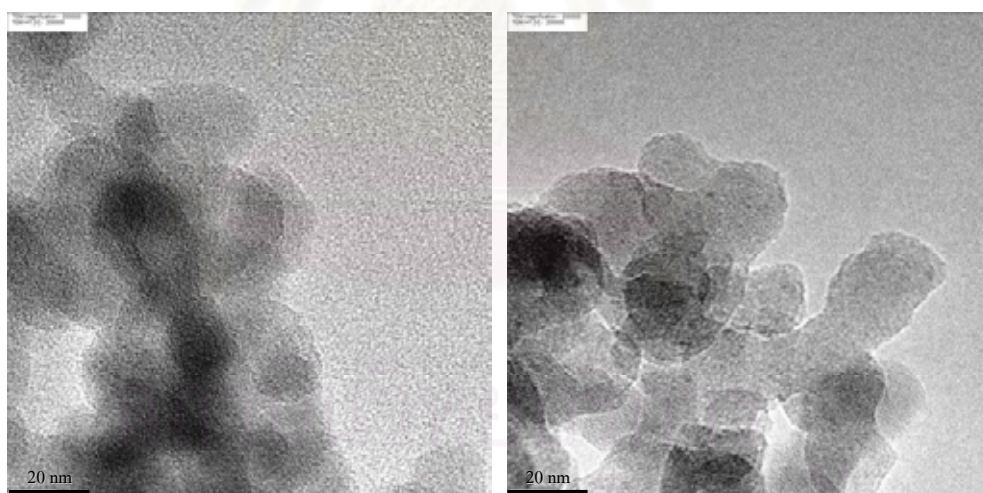
Figure 5.5   TEM micrographs of Pd/SiO$_2$-FSP catalyst with Pd loading 0.5 wt%
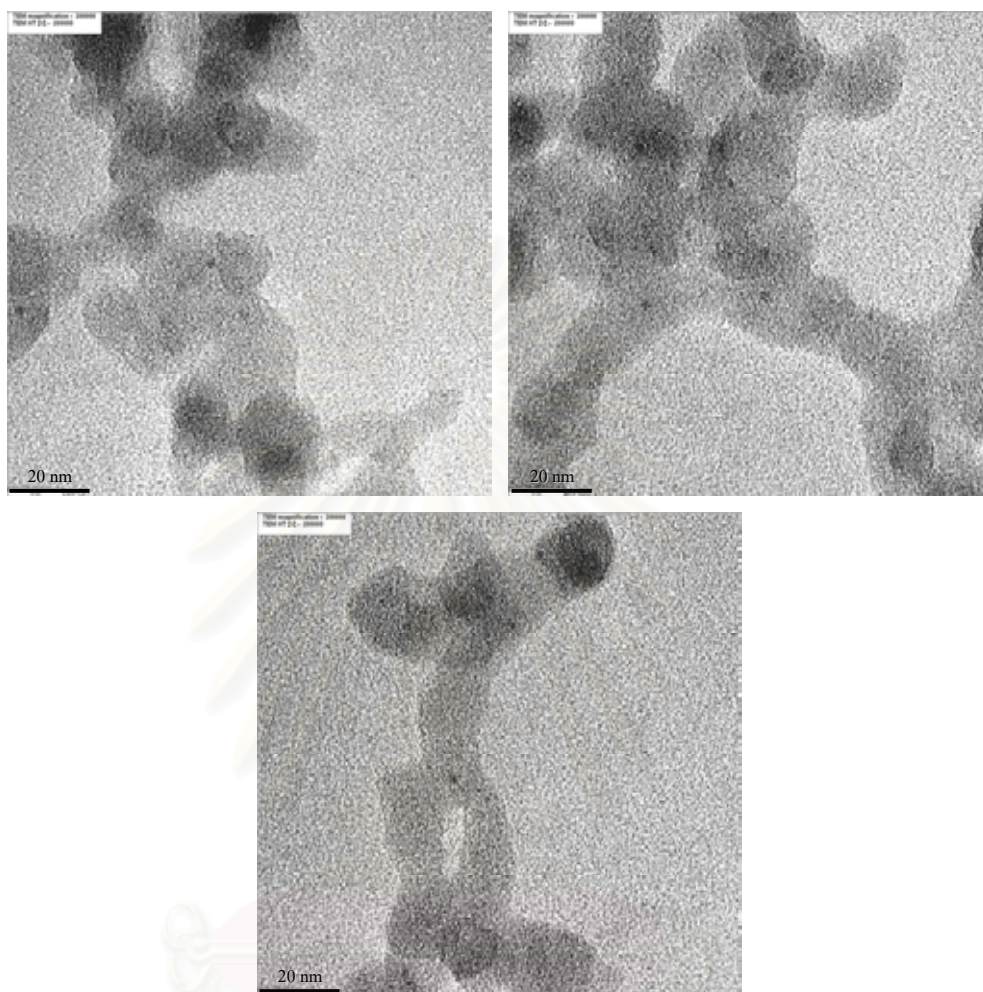
Figure 5.6   TEM micrographs of Pd/SiO$_2$-FSP catalyst with Pd loading 1 wt%
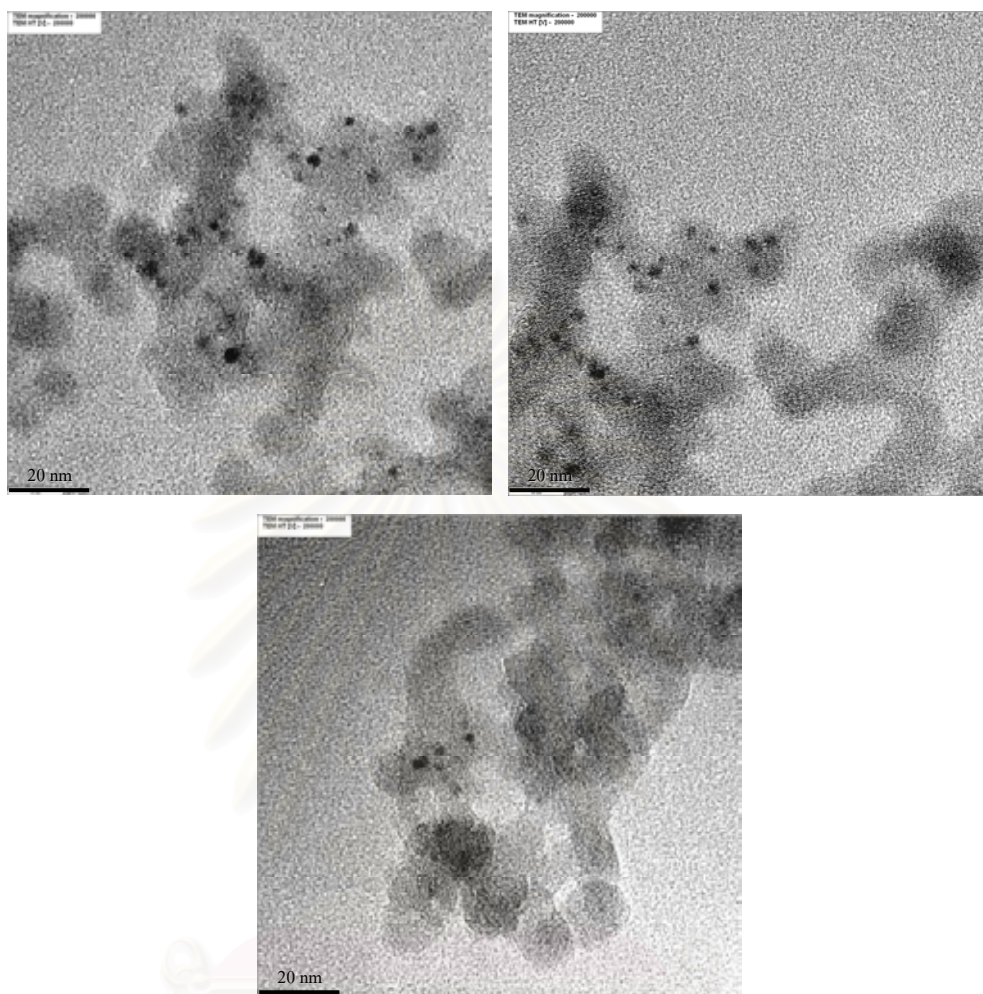
Figure 5.7   TEM micrographs of Pd/SiO$_2$-FSP catalyst with Pd loading 2 wt%
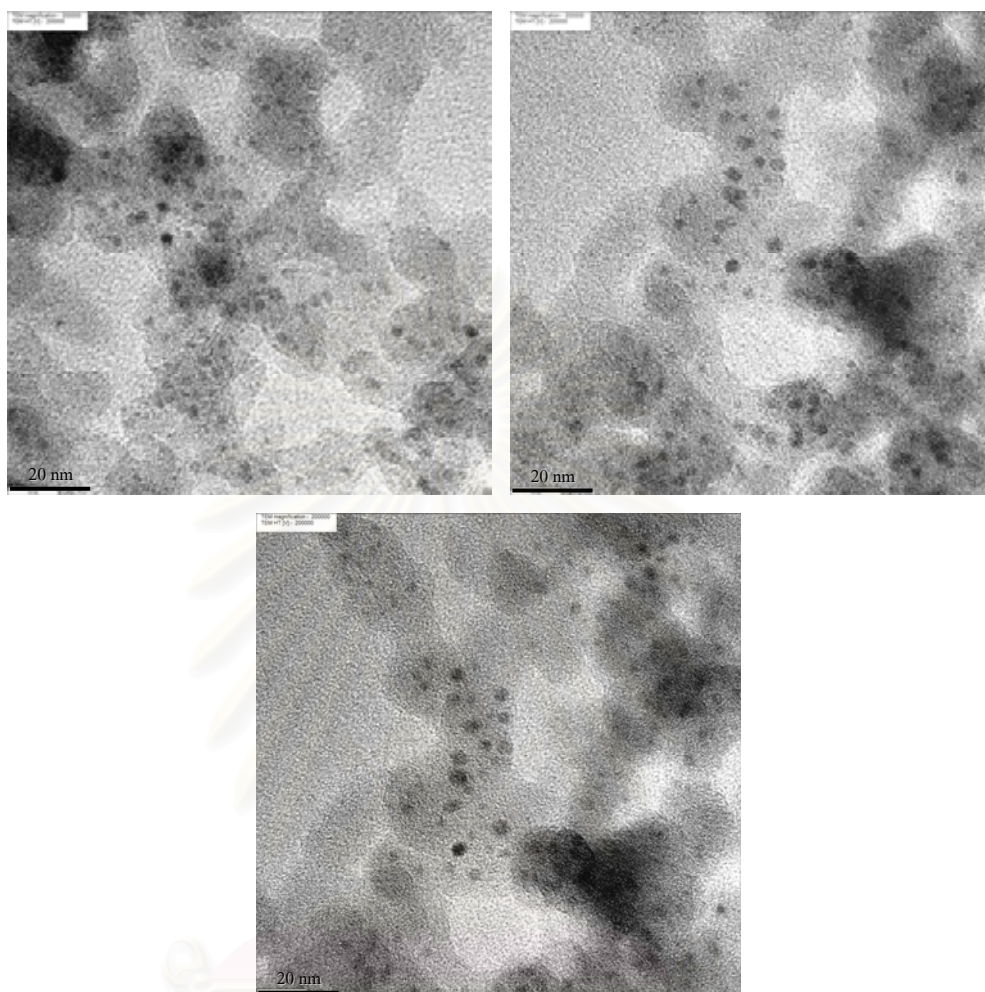
Figure 5.8   TEM micrographs of Pd/SiO$_2$-FSP catalyst with Pd loading 5 wt%
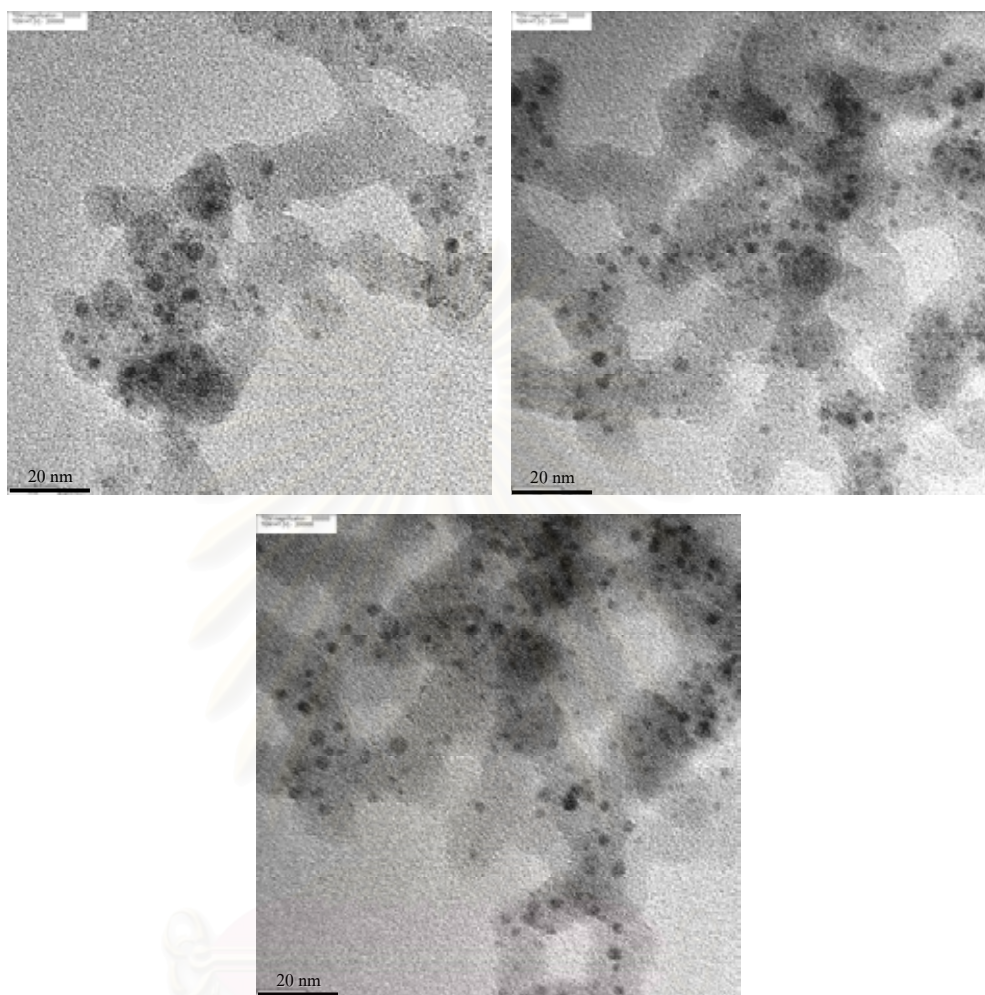
Figure 5.9   TEM micrographs of Pd/SiO$_2$-FSP catalyst with Pd loading 10 wt%
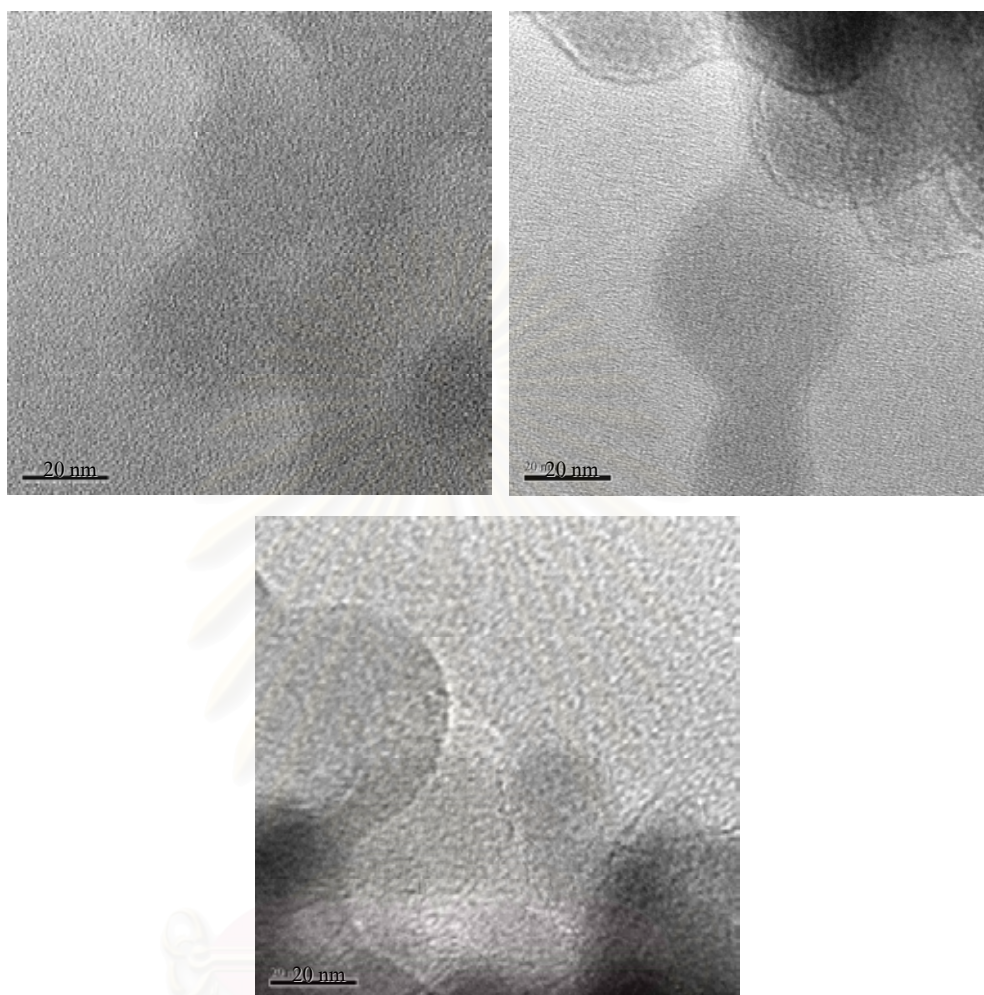
Figure 5.10   TEM micrographs of Pd/SiO$_2$-FSP-im catalyst with Pd loading 0.5 wt%
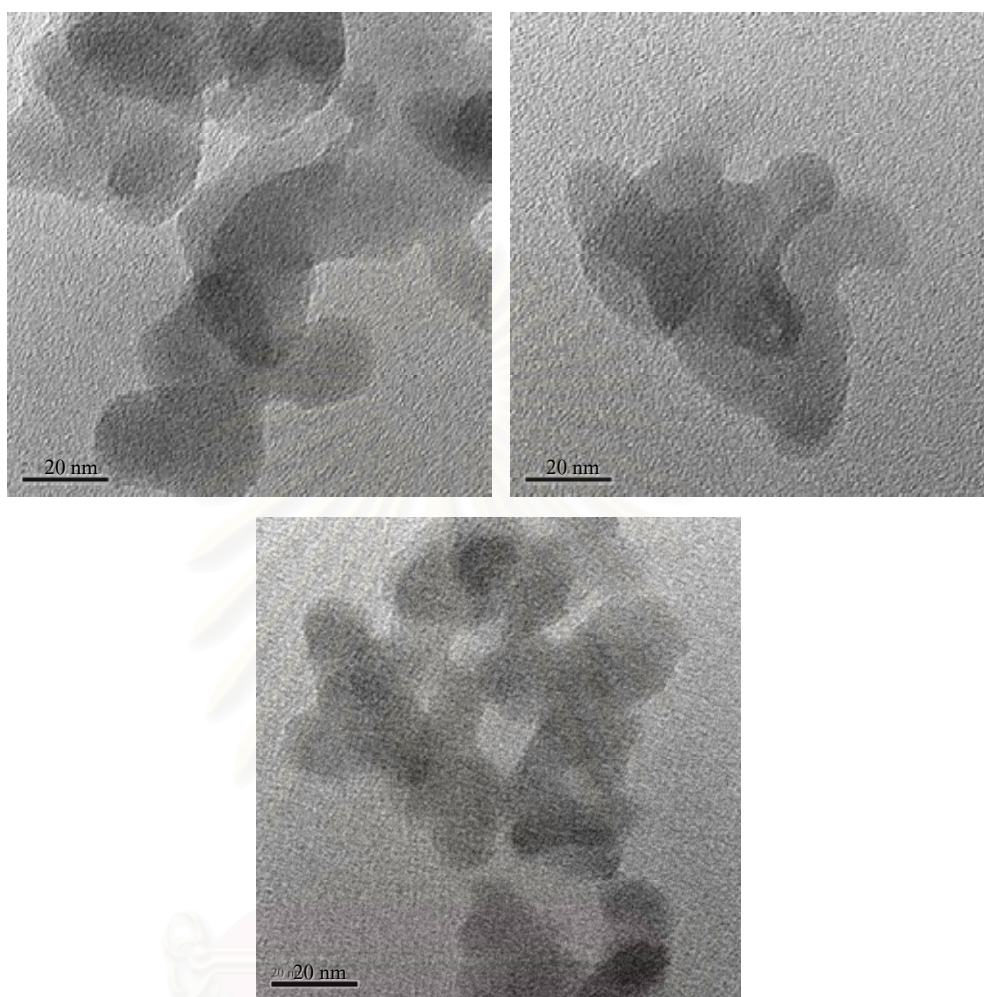
Figure 5.11   TEM micrographs of Pd/SiO$_2$-FSP-im catalyst with Pd loading 1 wt%
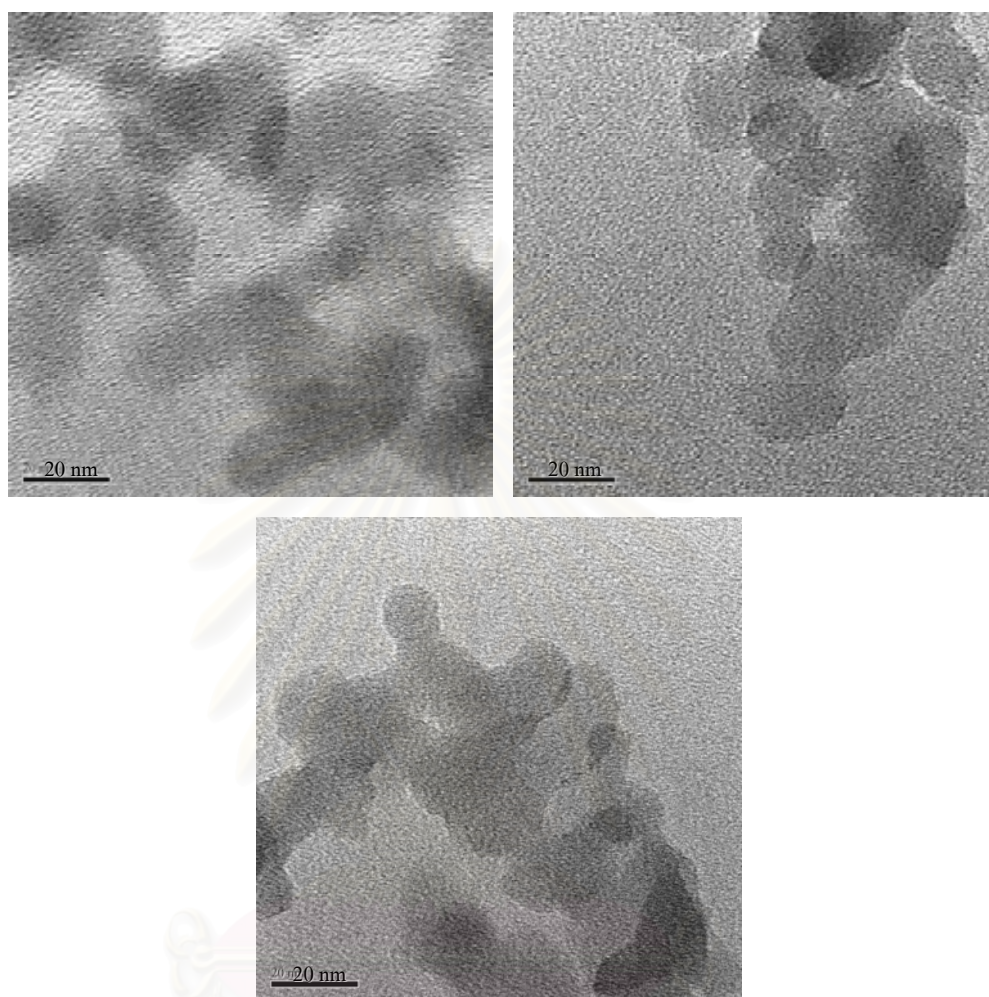
Figure 5.12   TEM micrographs of Pd/SiO$_2$-FSP-im catalyst with Pd loading 2 wt%
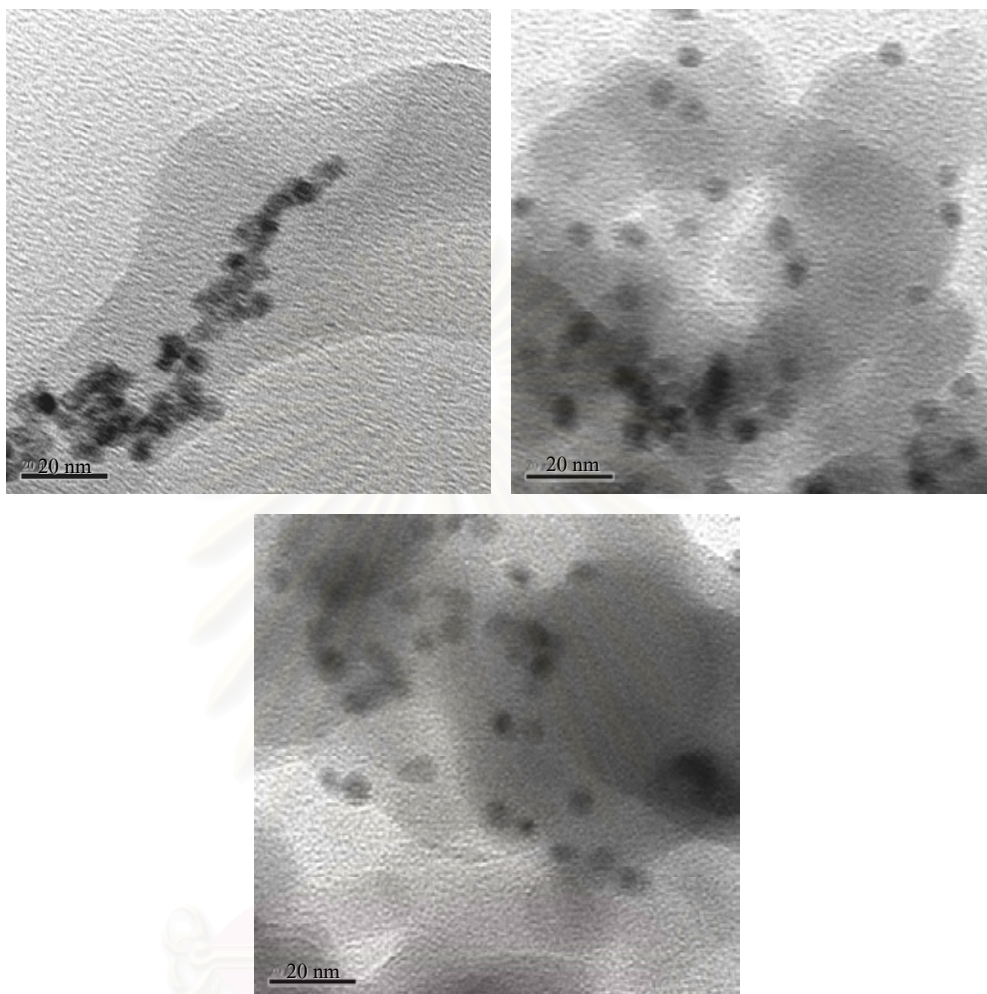
Figure 5.13   TEM micrographs of Pd/SiO$_2$-FSP-im catalyst with Pd loading 5 wt%
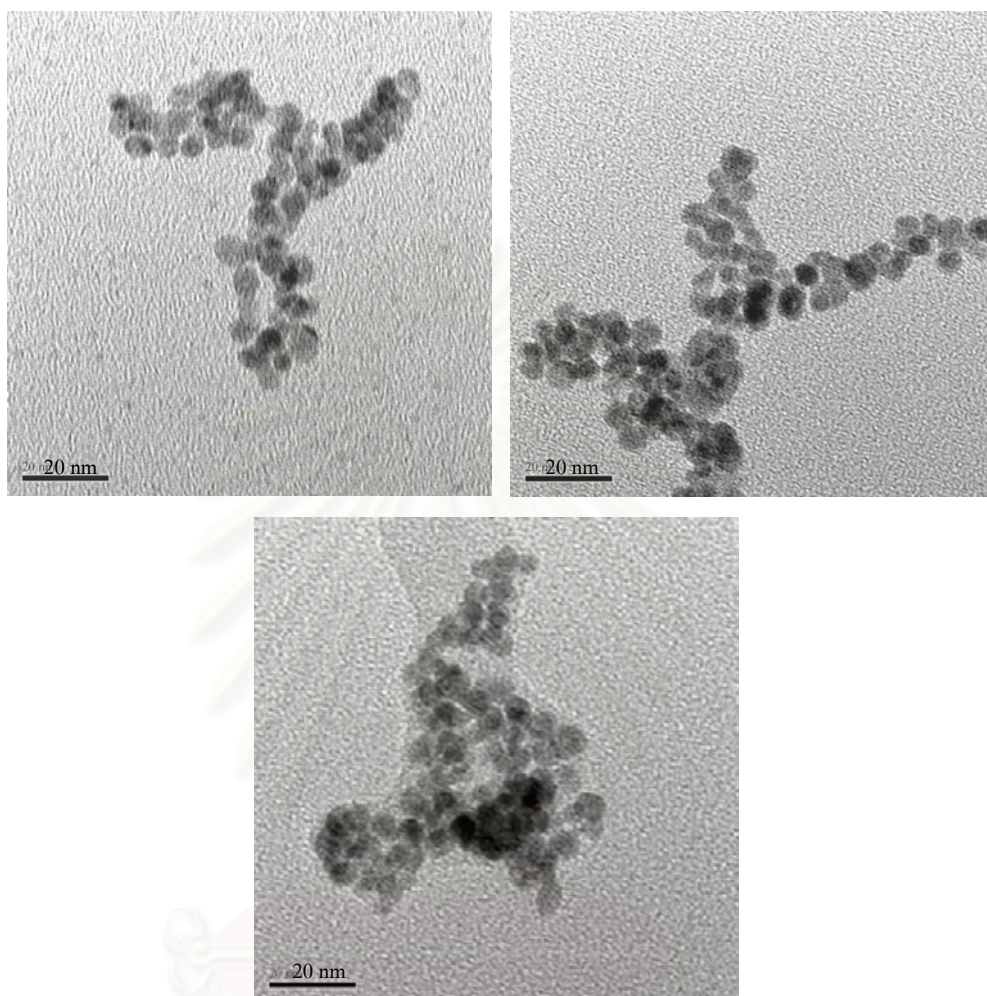
Figure 5.14   TEM micrographs of Pd/SiO$_2$-FSP-im catalyst with Pd loading 10 wt%

For TEM micrographs, the Pd diameter of the flame-made catalysts compared with that of the impregnated catalysts were not significantly different. The Pd metal peak from the XRD pattern of 5 wt% Pd/SiO$_2$-FSP was not found while the XRD pattern of 5 wt% Pd/SiO$_2$-FSP-im showed the peak of Pd metal. It may be due to well-dispersed Pd particles/clusters of the flame-made catalysts and/or the small Pd particles/clusters covered the formation of Si-O groups.

5.1.3   N$_2$ Physisorption

BET surface areas, pore volumes, and pore diameters of the flame-derived catalysts determined from N$_2$ physisorption technique are shown in Table 5.1. The particle formation process of silica-supported Pd catalysts is illustrated in Figure 2.1 (Chapter 2). The vapor pressure of silica was much lower than that of Pd/PdO in the hot flame environments, and consequently silica particle formation started earlier. Further the downstream flame, at lower temperatures, Pd/PdO started to form small particles and/or deposited directly on the SiO$_2$ support. This particle formation mechanism was also suggested for Pd/Al$_2$O$_3$ and Pt/ Al$_2$O$_3$ [32, 33]. The BET surface area of flame-made Pd/SiO$_2$ catalysts increased from 196 to 305 m^2/g as the amounts of Pd increased from 0 to 5 wt% and slightly decreased until 10 wt% Pd loading. It is suggested that the growth of the SiO$_2$ particles were inhibited by Pd dopant. This result is in good agreement with the works reported by Hannemann et al [21]. Average pore volume of the flame-made catalysts increased with increasing Pd loading and was determined to be 0.43 – 0.69 cm^3/g.

The N$_2$ adsorption – desorption isotherms of the flame-made catalyst with Pd loading 0 – 10 wt% are shown in Figure 5.15 to Figure 5.20, respectively. The pore size distribution patterns are shown in Figure 5.21. According to the calculation using BJH desorption equation, it indicates the pattern for mesopore structure (type IV isotherm). The average pore diameters were nearly constant for the flame-made Pd/SiO$_2$ catalysts with 0.5 – 5 wt% while the average pore size of 10 wt% Pd/SiO$_2$ increased slightly.

The results from N$_2$ physisorption technique such as the BET surface area, the pore volumes, and the pore sizes of the impregnated catalysts are shown in Table 5.2. The BET surface area of flame-made silica was 196 m^2/g. When Pd loading increased from 0.5 to 5 wt%, the BET surface areas decreased from 174 to 109 m^2/g and the BET surface area increased as Pd contents increased from 5 to 10 wt%. Decreasing on BET surface area can be explained by sintering occurred in calcination process and pore blockage of PdO cluster. Average pore volumes of impregnated catalysts decreased from 0.91 to 0.47 cm^3/g with increasing Pd loading between 0.5 to 5 wt% and relatively constant when Pd loading increased to 10 wt%.

Figure 5.22 to Figure 5.26 show the N$_2$ adsorption – desorption isotherms of the FSP-im catalyst and the pore size distribution patterns are shown in Figure 5.27

calculated by BJH desorption equation that indicated the pattern for mesopore structure (type IV isotherm). The average pore sizes of impregnated catalysts with various Pd loadings were not different.

Table 5.1 N_2 physisorption properties of the flame-made catalysts

Catalyst	N_2 Physisorption		
	BET surface area (m²/g)	Pore Volume (cm³/g)	Average Pore Diameter (nm)
SiO$_2$	196	0.48	9.0
0.5%Pd/SiO$_2$-FSP	246	0.43	6.7
1%Pd/SiO$_2$-FSP	251	0.46	7.4
2%Pd/SiO$_2$-FSP	260	0.49	7.8
5%Pd/SiO$_2$-FSP	306	0.59	7.6
10%Pd/SiO$_2$-FSP	299	0.69	9.1
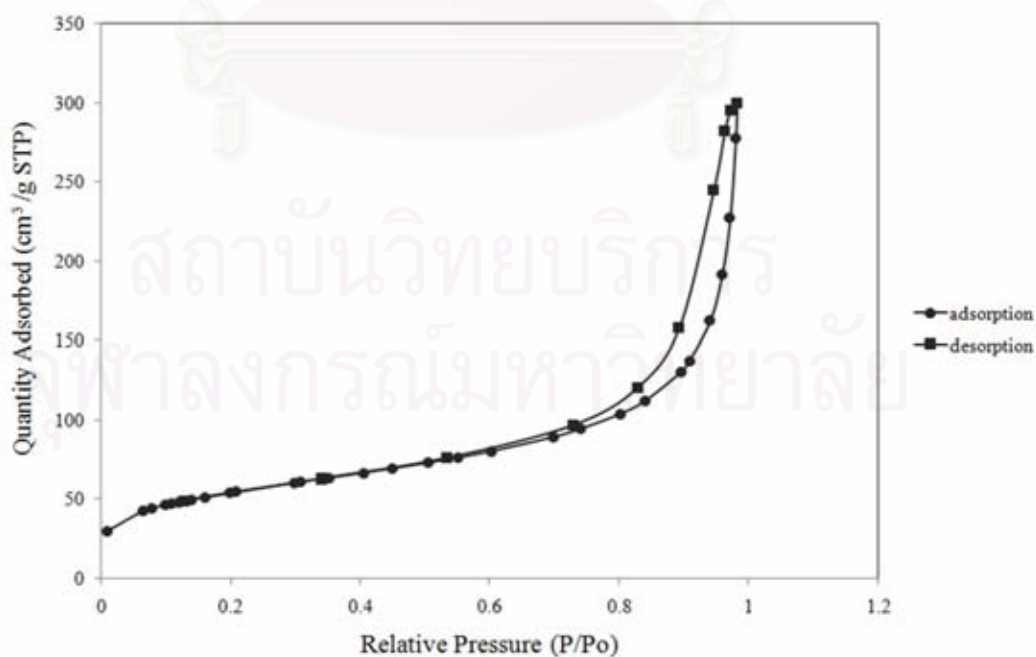
Figure 5.15 N_2 adsorption – desorption isotherms of FSP silica
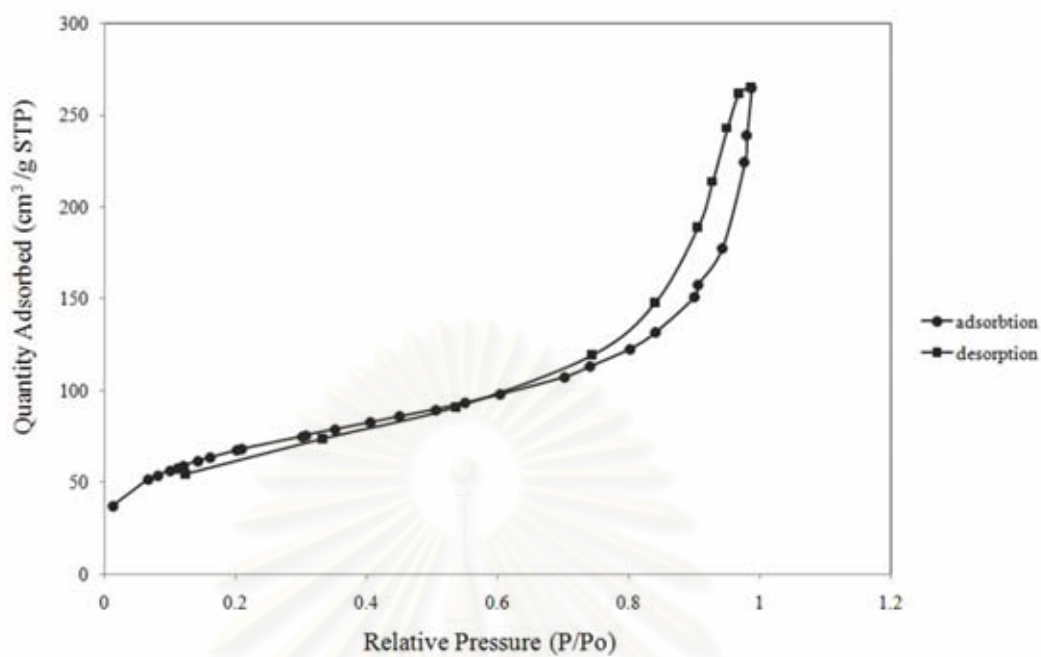
Figure 5.16 N$_2$ adsorption – desorption isotherms of 0.5 wt% Pd/SiO$_2$-FSP
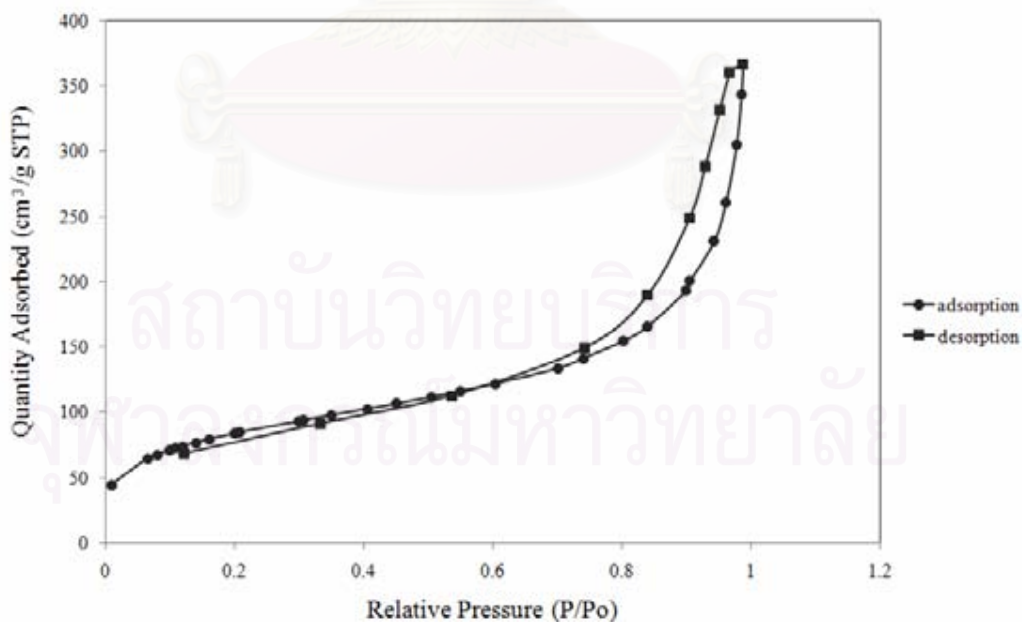
Figure 5.17 N$_2$ adsorption – desorption isotherms of 1 wt% Pd/SiO$_2$-FSP
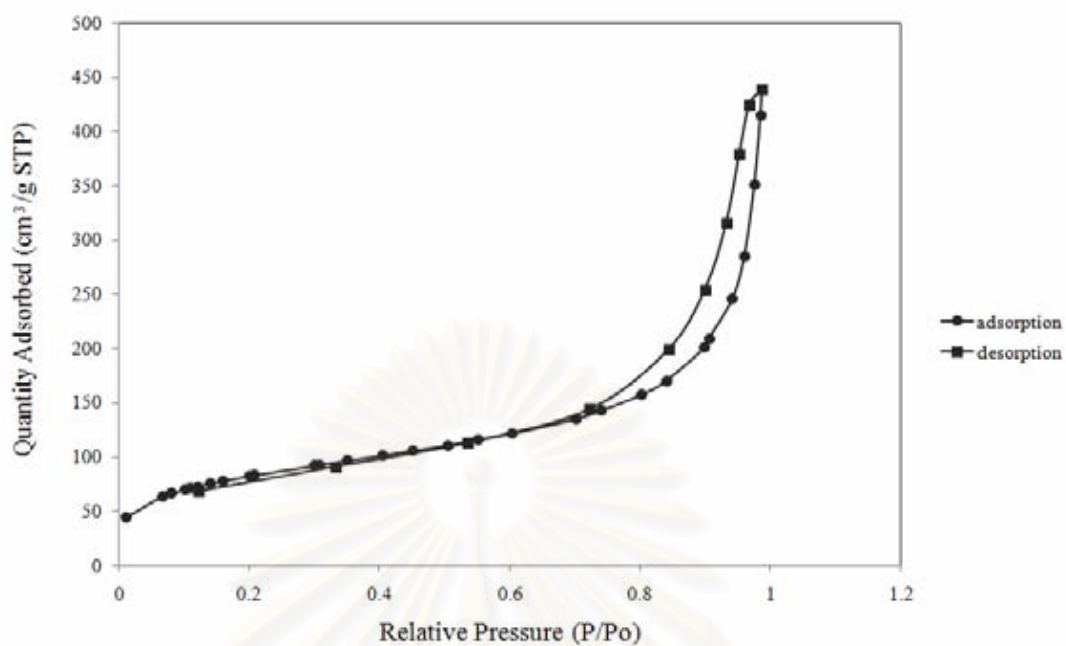
Figure 5.18 N$_2$ adsorption – desorption isotherms of 2 wt% Pd/SiO$_2$-FSP
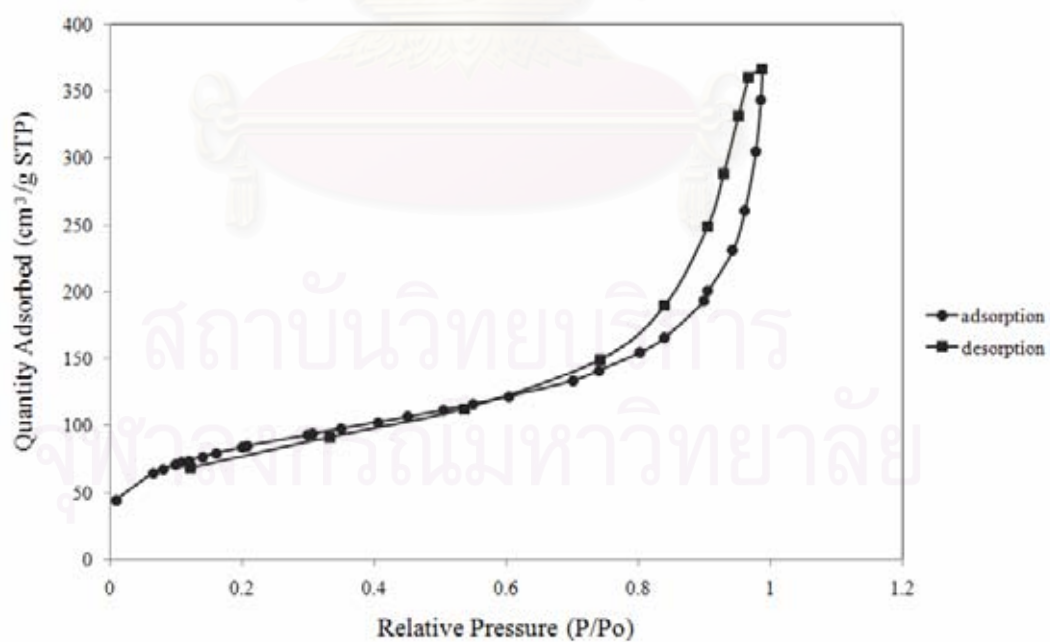
Figure 5.19 N$_2$ adsorption – desorption isotherms of 5 wt% Pd/SiO$_2$-FSP
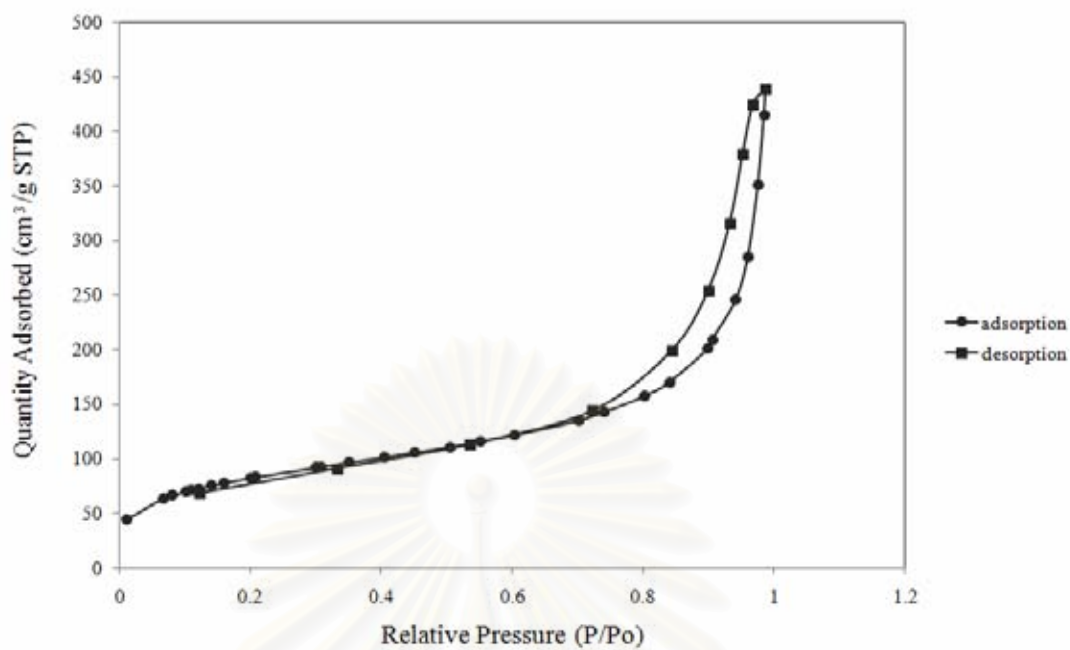
Figure 5.20   N$_2$ adsorption – desorption isotherms of 10 wt% Pd/SiO$_2$-FSP
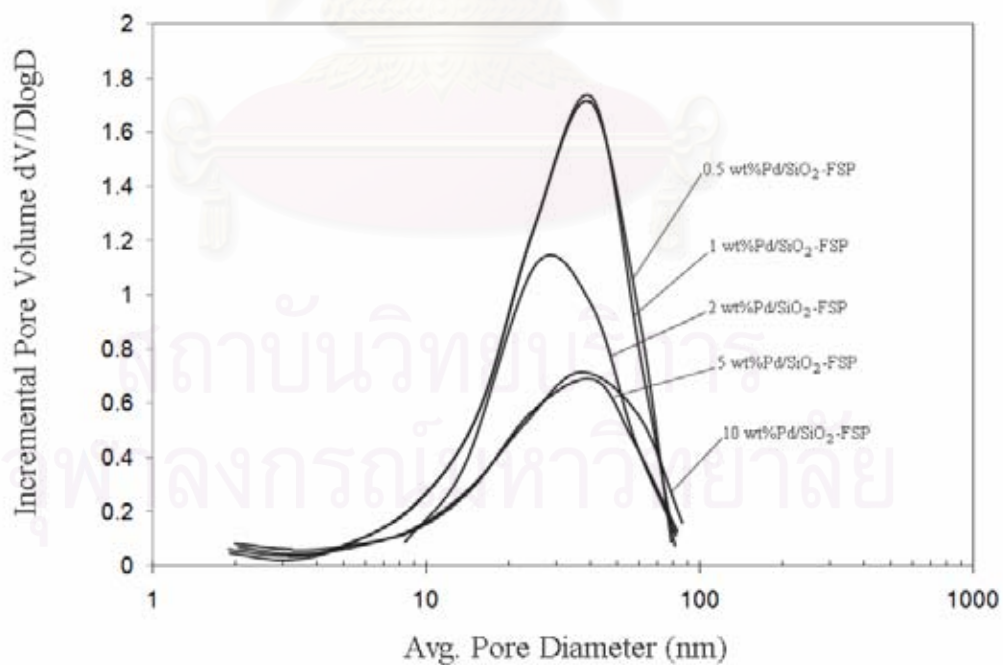
Figure 5.21   Pore size distribution of flame-made catalysts

Table 5.2 N_2 physisorption properties of the impregnated catalysts

Catalyst	N_2 Physisorption		
	BET surface area (m^2/g)	Pore Volume (cm^3/g)	Average Pore Diameter (nm)
0.5%Pd/SiO$_2$-FSP-im	174	0.91	20.4
1%Pd/SiO$_2$-FSP-im	171	0.91	19.4
2%Pd/SiO$_2$-FSP-im	133	0.60	24.9
5%Pd/SiO$_2$-FSP-im	109	0.47	14.4
10%Pd/SiO$_2$-FSP-im	128	0.50	16.8
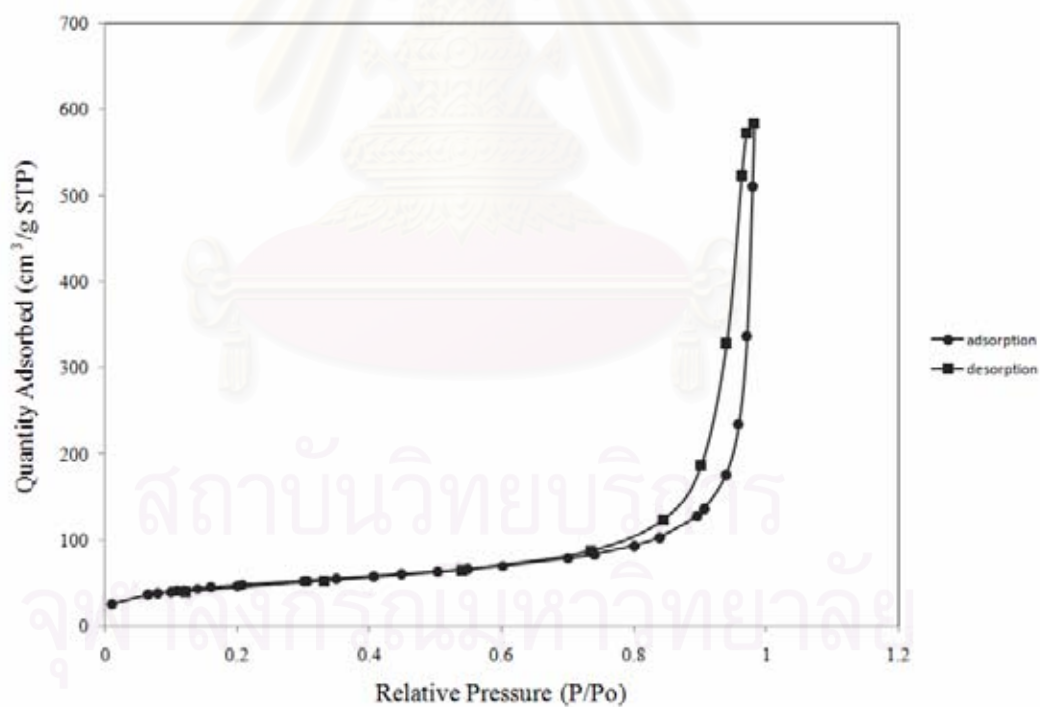
Figure 5.22 N_2 adsorption – desorption isotherms of 0.5 wt% Pd/SiO$_2$-FSP-im
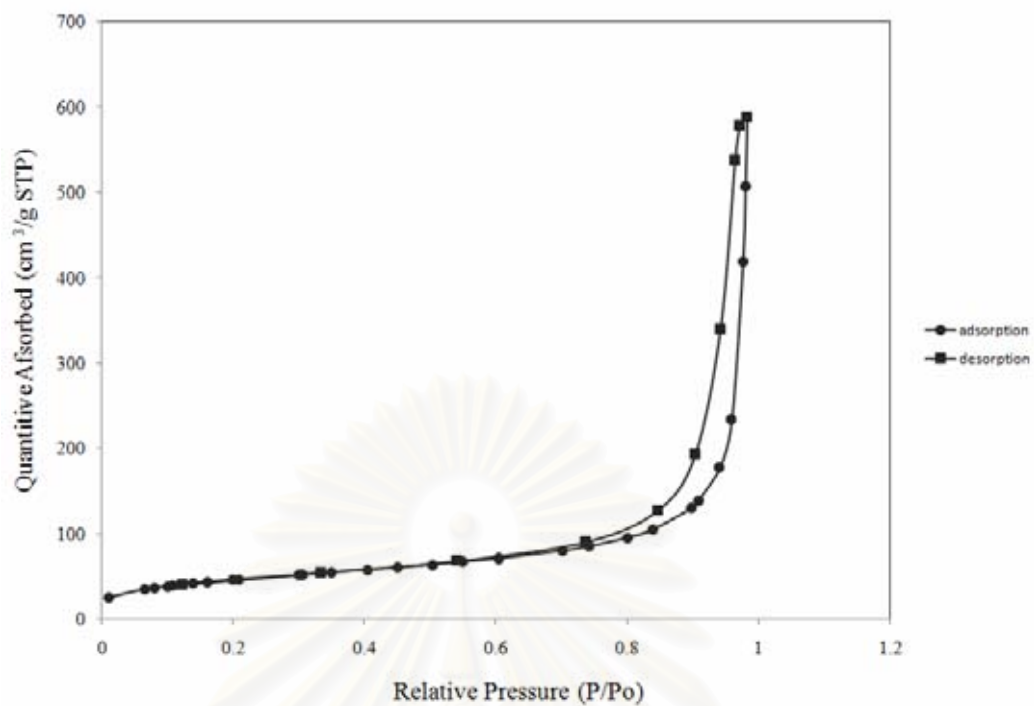
Figure 5.23 N$_2$ adsorption – desorption isotherms of 1 wt% Pd/SiO$_2$-FSP-im
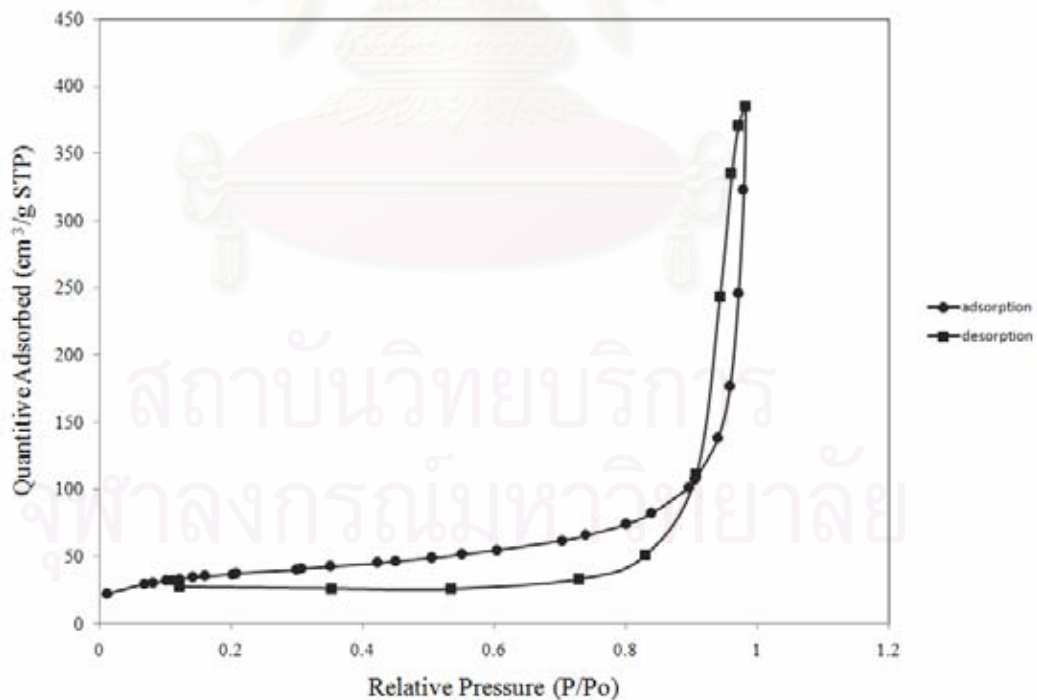
Figure 5.24 N$_2$ adsorption – desorption isotherms of 2 wt% Pd/SiO$_2$-FSP-im
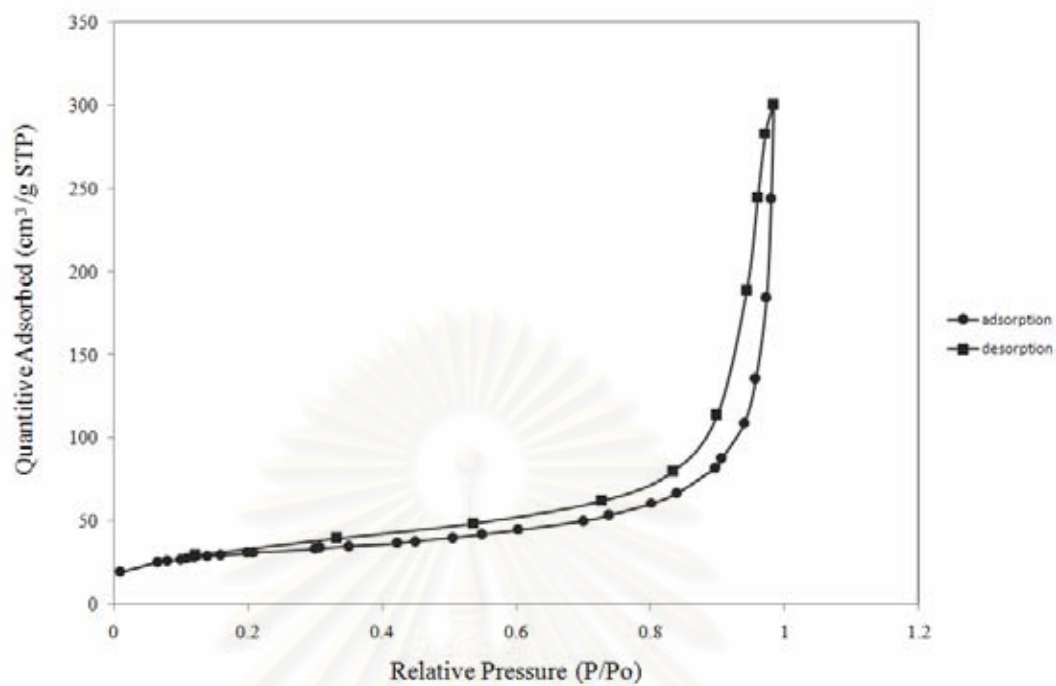
Figure 5.25 N_2 adsorption – desorption isotherms of 5 wt% Pd/SiO$_2$-FSP-im
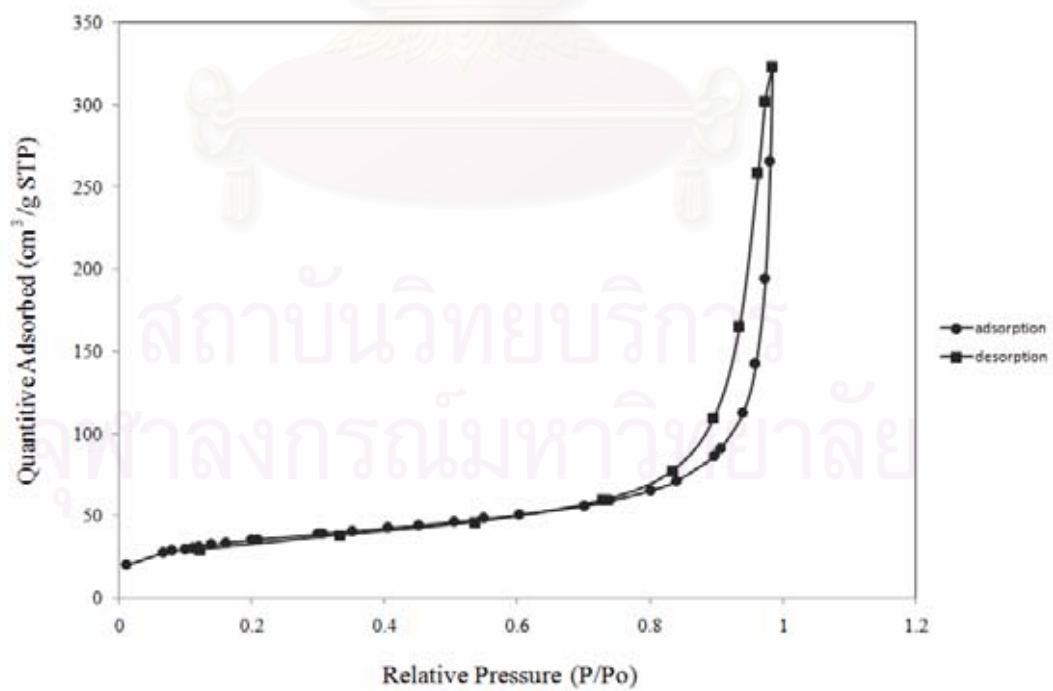
Figure 5.26 N_2 adsorption – desorption isotherms of 10 wt% Pd/SiO$_2$-FSP-im
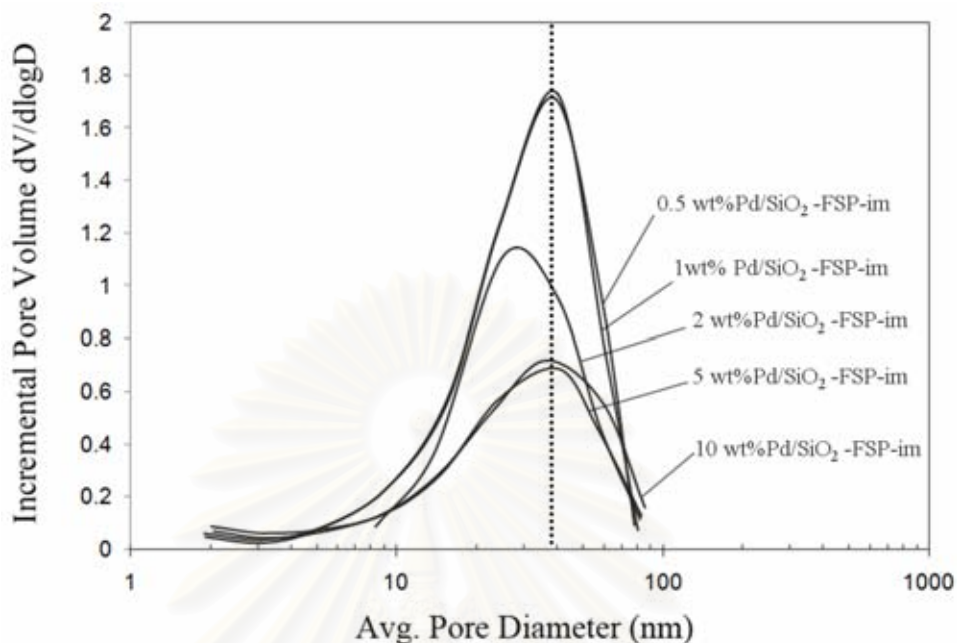
Figure 5.27   Pore size distribution of the impregnated catalysts

The BET surface areas of the flame-made catalysts increased from 0.5 to 5 wt% as those of the impregnated catalysts decreased. Decreasing of the BET surface areas with increasing metal loading is typical for supported metal catalysts prepared by conventional impregnation method. It was probably due to sintering during the calcinations process and pore blockage of Pd/PdO clusters. For the flame-made catalysts, it suggests that the Pd dopants inhibited the growth of SiO_2 particle resulting in an increase in BET surface area with increasing Pd loading.

5.1.4   CO-pulse chemisorptions

The relative amounts of active surface Pd metal on the catalyst samples were calculated from CO chemisorption experiments at room temperature. The calculation of Pd active sites was based on the assumption that one carbon monoxide molecule adsorbs on one palladium site [33, 36]. The active sites increased from 0.97×10^{18} to 25.84×10^{18} site/g-catalyst corresponding to the increasing in %Pd metal dispersion

from 3.4 to 4.6% as the Pd contents increased from 0.5 to 10 wt%. The average Pd^0 metal particle sizes calculated from CO chemisorption were found to be 24 – 40 nm. The particle sizes were much larger than those based on TEM analyses.

The low metal dispersion and overestimation of metal particle sizes in supported Pd catalysts based on CO chemisorptions may be due to the formation of Si-O groups covering the small palladium particles. This was inhibited the adsorption of CO molecules, so the CO chemisorptions uptake decreased. Otherwise, CO chemisorptions suppression may be due to strong interactions between Si and Pd in an alloy form.

The amounts of CO chemisorption on the impregnated catalysts are given in Table 5.4. The active sites increased from 3.78×10^{18} to 27.8×10^{18} site/g catalyst corresponding to the increasing Pd contents from 0.5 to 10 wt% as Pd metal dispersion decreased from 13.4% to 4.9%. The Pd^0 metal particle sizes calculated from CO chemisorption were found to be increased from 8 to 23 nm as Pd loading 0.5-10 wt%.

The amounts of CO chemisorption on the reference catalysts are given in Table 5.4. The amounts of CO chemisorption increased in the order of Lindlar > 2%Pd/ SiO_2-com > 1%Pd/ SiO_2-com > 0.5%Pd/ SiO_2-com. The palladium dispersion of Pd/ SiO_2 catalysts prepared by ion-exchange method were nearly constant as the amount of CO chemisorption increased with increasing Pd content between 0.5 and 2 wt% and the sizes of Pd metal were constant. For Lindlar catalysts, the Pd dispersion was lower than Pd/SiO_2-com but larger Pd metal particle than Pd/SiO_2-com that resulted in low Pd dispersion. However, the Lindlar catalyst exhibited higher CO chemisorptions uptake.

Table 5.3   The amounts of CO chemisorption

Catalyst	CO uptake ($\times 10^{-18}$ molecule CO/g-catalyst)	%Pd dispersion[a]	$d_pPd^{0,a}$ (nm)
0.5%Pd/SiO$_2$-FSP	1.0	3.42	33
1%Pd/SiO$_2$-FSP	1.9	3.40	33
2%Pd/SiO$_2$-FSP	3.3	2.88	39
5%Pd/SiO$_2$-FSP	13.4	4.71	24
10%Pd/SiO$_2$-FSP	25.8	4.55	25
0.5%Pd/SiO$_2$-FSP-im	3.79	13.4	8
1%Pd/SiO$_2$-FSP-im	5.02	8.87	13
2%Pd/SiO$_2$-FSP-im	7.70	6.80	16
5%Pd/SiO$_2$-FSP-im	17.99	6.36	18
10%Pd/SiO$_2$-FSP-im	27.80	4.91	23
0.5%Pd/SiO$_2$-com	1.90	6.72	17
1%Pd/SiO$_2$- com	5.17	9.14	12
2%Pd/SiO$_2$- com	7.89	6.97	16
Lindlar	10.4	3.68	30

[a] Based on the total palladium loaded

5.1.5   X-ray Photoelectron Spectroscopy (XPS)

XPS is a powerful tool for determination of the composition of the catalyst and the interaction between Pd and silica supports. The elemental scans for each component on the surface of the silica-supports palladium catalysts prepared by flame spray pyrolysis and the impregnated catalysts are shown in Figure 5.28 and Figure 5.29, respectively and summarized in Table 5.5.

For the flame-made catalyst with 0.5 – 2 wt% Pd loading, Pd $3d_{5/2}$ peaks were not observed. It is suggested that very low amount of Pd present on the surface of catalysts. For 5 and 10 wt% Pd/SiO_2, the binding energy of Pd $3d_{5/2}$ was 337.4 eV which was higher energy comparing to Pd^0 (335.1 eV) [37], and higher than Pd $3d_{5/2}$ on the classic Lindlar catalysts according to the literature [38, 39]. From the results, the electron-deficient Pd in flame-made Pd/SiO_2 catalyst was obtained directly from flame process. This indication supports the results of CO chemisorption.

The FWHM values, higher than 2.0 eV, are also indicative that more than one Pd species may be present in the flame-derived catalyst as have been suggested for Pd/Al_2O_3 and Pd/C catalysts prepared by conventional impregnation technique [39].

The percentages of atomic concentration for Si 2p, O 1s, and Pd 3d are also given in Table 5.5. For the catalysts with Pd loading 0.5 – 2 wt%, much lower Pd/Si ratios were observed. It is in good agreement with the CO chemisorption results for the catalysts with relative low metal loadings. The lower Pd/Si ratios suggests that large amount of Pd existed deep inside the pore of the supports rather than on the outer surface. The metal surface may be covered by Si-O groups due to simultaneous crystallization of Pd and SiO_2 in gas-phase during FSP.

For the reduced-impregnated catalysts, the Pd $3d_{5/2}$ peaks with Pd content 0.5-2 wt% were not observed probably due to very low amount of Pd present on the surface. The Pd 3d binding energies of 5 and 10 wt% impregnated Pd catalysts ranged around 335.7 eV which was in good agreement with Pd^0 (335.1 eV). It is indicated that there was less interaction between Pd and SiO_2 supported on these catalysts.

The Pd/Si ratios for impregnated catalysts increased with increasing Pd content from 0.5 to 10 wt% suggesting that for low Pd loading most of the palladium existed deep inside the pore of the supports rather than on the outer surface. The XPS results are in good agreement with the CO chemisorption results.
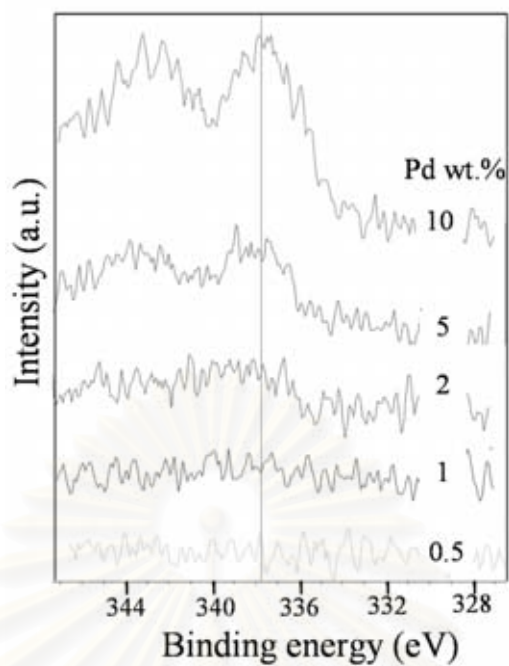
Figure 5.28 XPS results of flame-made catalysts with 0 – 10 wt% Pd loading
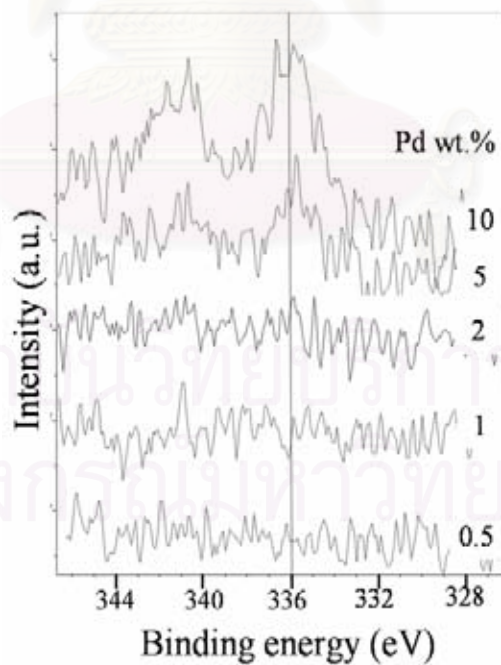
Figure 5.29 XPS results of reduced-impregnated catalysts with 0 – 10 wt% Pd loading

Table 5.4   XPS results Pd $3d_{5/2}$ of the catalysts

Catalyst	XPS results Pd $3d_{5/2}$		Atomic ratio
	B.E. (eV)	FWHM	Pd/Si
0.5%Pd/SiO$_2$-FSP	n/a	n/a	0.0011
1%Pd/SiO$_2$-FSP	n/a	n/a	0.0014
2%Pd/SiO$_2$-FSP	n/a	n/a	0.0018
5%Pd/SiO$_2$-FSP	337.4	2.389	0.0139
10%Pd/SiO$_2$-FSP	337.4	3.189	0.0404
0.5%Pd/SiO$_2$-FSP-im	n/a	n/a	0.0011
1%Pd/SiO$_2$-FSP-im	n/a	n/a	0.0020
2%Pd/SiO$_2$-FSP-im	n/a	n/a	0.0024
5%Pd/SiO$_2$-FSP-im	335.7	1.109	0.0056
10%Pd/SiO$_2$-FSP-im	335.8	1.744	0.0142

5.2 Reaction Study

The catalytic behavior of the flame-made catalysts was investigated in liquid-phase selective hydrogenation in a batch system in a 50 ml autoclave reactor. The reaction was operated with high stirring rate (1000 rpm) in order to eliminate the external mass transfer of hydrogen problem. The reaction was carried out using 2% v/v heptyne in toluene at 30°C and 1 bar H$_2$ pressure. The products were analyzed by gas chromatography with flame ionization detector (FID) using GS-alumina column.

The conversions and selectivities of all FSP catalysts are presented in Table 5.6. The conversion of 1-heptyne increased from 42 to 75% with increasing Pd loading from 0.5 to 5 wt% and remained relatively constant when Pd loading was increased to 10 wt%. The selectivities for 1-heptene were higher than 90% for all the FSP catalysts.

The catalytic performance in terms of the turnover frequencies (TOFs) were calculated using the amounts of surface metal atoms measured by CO chemisorption and given in Table 5.7. The specific activity (TOF) is defined as mole of product/mole of metal/time. For the increasing palladium loading between 0.5 and 10 wt%, the TOFs of the flame-made catalysts decreased from 66.2 to 4.3 s^{-1}. The high TOF values for the flame-made catalysts with low Pd loading ($\leq$ 2 wt%) can be explained by CO chemisorption suppression on these catalysts. It may be due to strong metal-support interaction. Furthermore, Pd metal surface may be covered by Si-O groups during flame spray synthesis. For the 10 wt% Pd/SiO$_2$, CO chemisorption suppression was not observed and most of the Pd was in metallic state as indicated by XRD. The TOF continuingly decreased from 2 to 10 wt% Pd loading while the diameters of Pd metal were similar. The remarkable high catalytic hydrogenation activities (TOFs) of Pd nanoparticles have also been reported of other Pd/SiO$_2$ systems [39, 40] with Pd particla size 1 – 2 nm.

The catalyst activities and selectivities for liquid-phase hydrogenation of 1-heptyne at 30°C in toluene are shown in Table 5.6. The hydrogenation activities show similar order to the CO chemisorption results that conversion increased with increading Pd loading from 0.5 to 10 wt%. The selectivities for 1-heptyne increased from 91 to 98% as the Pd content to 10 wt%. The 1-heptyne hydrogenation activities in terms of turnover frequencies (TOFs) are shown in Table 5.7. While Pd loading increased from 0.5 to 10 wt% the TOF values of impregnated Pd/SiO$_2$ catalysts remained constant around 2-6 s^{-1}.

The catalytic performance in terms of 1-heptyne conversions and selectivities to 1-heptene and the turnover frequencies calculated based on CO chemisorption results are given in Table 5.6 and 5.7, respectively. The conversions of 1-heptyne on the reference catalysts increased from 21% to 60% as the CO chemisorption results increased while the selectivities to 1-heptene increased slightly from 94% to 97%. The TOF values were quite similar (3.3 – 8.5 s^{-1}).

Table 5.5   Results of 1-heptyne hydrogenation

Catalyst	Conversion (%)	Selectivity (%)	
		to 1-heptene	to n-heptane
0.5%Pd/SiO_2-FSP	42	93	7
1%Pd/SiO_2-FSP	43	92	8
2%Pd/SiO_2-FSP	54	94	6
5%Pd/SiO_2-FSP	75	95	5
10%Pd/SiO_2-FSP	73	94	6
0.5%Pd/SiO_2-FSP-im	13	91	9
1%Pd/SiO_2-FSP-im	21	95	5
2%Pd/SiO_2-FSP-im	32	96	4
5%Pd/SiO_2-FSP-im	48	96	4
10%Pd/SiO_2-FSP-im	52	98	2
0.5%Pd/SiO_2-com	21	94	6
1%Pd/SiO_2- com	27	94	6
2%Pd/SiO_2- com	31	95	5
Lindlar	60	97	3

Table 5.6   TOFs of the catalysts

Catalyst	TOF (s^{-1})
0.5%Pd/SiO$_2$-FSP	66.2
1%Pd/SiO$_2$-FSP	34.1
2%Pd/SiO$_2$-FSP	25.3
5%Pd/SiO$_2$-FSP	8.6
10%Pd/SiO$_2$-FSP	4.3
0.5%Pd/SiO$_2$-FSP-im	5.2
1%Pd/SiO$_2$-FSP-im	6.4
2%Pd/SiO$_2$-FSP-im	6.4
5%Pd/SiO$_2$-FSP-im	4.1
10%Pd/SiO$_2$-FSP-im	2.9
0.5%Pd/SiO$_2$-com	8.5
1%Pd/SiO$_2$- com	8.2
2%Pd/SiO$_2$- com	6.2
Lindlar	3.3

For similar low Pd content, it was found that the catalysts prepared by one-step FSP method exhibited higher 1-heptyne conversion than the impregnated catalysts and reference catalysts. While comparing Pd/SiO$_2$-com and Pd/SiO$_2$-FSP-im with similar Pd loading (0.5-2 wt%), the catalysts showed similar 1-heptyne conversions. It may be due to the smaller pore volumes of the flame-made catalysts than those of others while the BET surface areas of the flame-made catalysts were higher than those of impregnated and Pd/SiO$_2$-com catalysts.

For the catalytic activities in term of TOF, it was found that the TOFs of the flame-made catalysts decreased from 66.2 to 4.3 s^{-1} with increasing Pd loading from 0.5 to 10 wt% whereas the TOFs of the impregnated and Pd/SiO$_2$-com catalysts varied between 3-9 s^{-1}. The TOFs of the flame-made catalysts especially those with

relatively low Pd content were higher than that of impregnated and reference catalyst. It is suggested that the formation of electron-deficient Pd species and strong Pd and SiO$_2$ interaction resulting in CO chemisorptions suppression and high TOF value. However, there was no effect on the selectivity to 1-heptene.

5.3 Catalyst Deactivation

Catalyst deactivation due to metal sintering was studied using TEM technique. TEM micrographs of the spent flame-made catalysts are shown in Figure 5.30 to Figure 5.34 and those of the spent impregnated catalysts are given in Figure 5.35 to Figure 5.39. Pd metal particles/clusters were still observed in spherical shape. Plot between Pd particle/cluster size and Pd contents of flame-made and impregnated catalysts are shown in Figure 5.40. The particle/cluster size of Pd metals of the flame-made catalysts slightly increased after reaction. It was probably due to the small Pd particle/cluster covered the Si-O group for the spent catalyst less than the fresh catalysts. So the flame-made catalyst did not find deactivation by metal sintering.

For the impregnated catalysts, the Pd particle/cluster diameters were slightly increased after reaction, suggesting due to the sintering process. However, the mechanism of metal sintering in liquid-phase reactions has not been well-investigated so far.
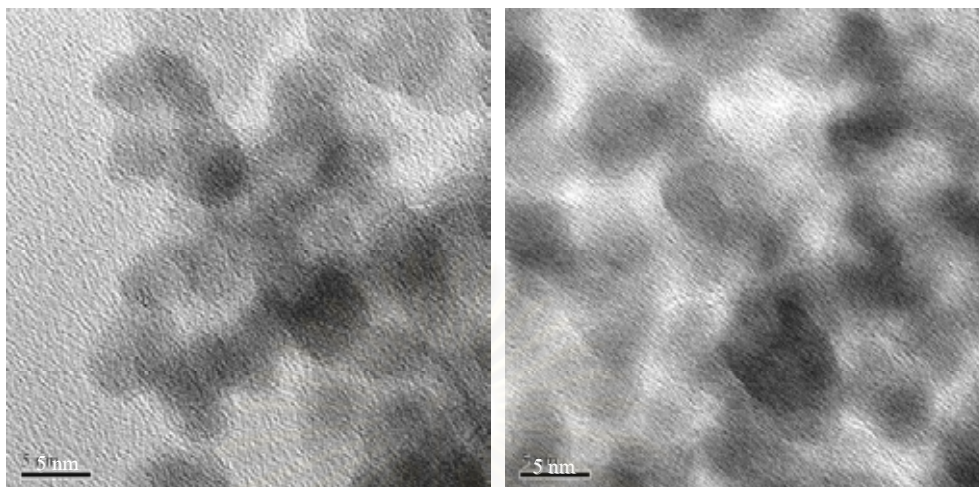
Figure 5.30   TEM micrographs of spent Pd/SiO$_2$-FSP with Pd loading 0.5 wt%
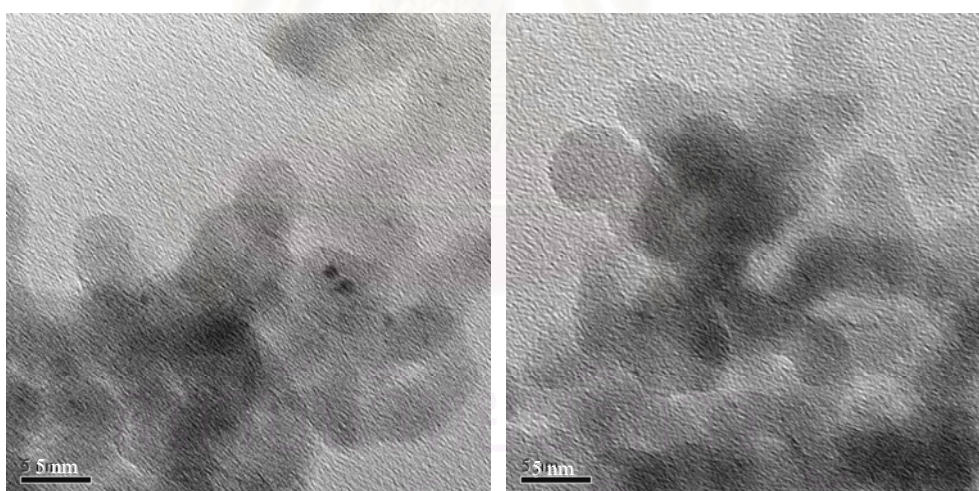
Figure 5.31   TEM micrographs of spent Pd/SiO$_2$-FSP with Pd loading 1 wt%
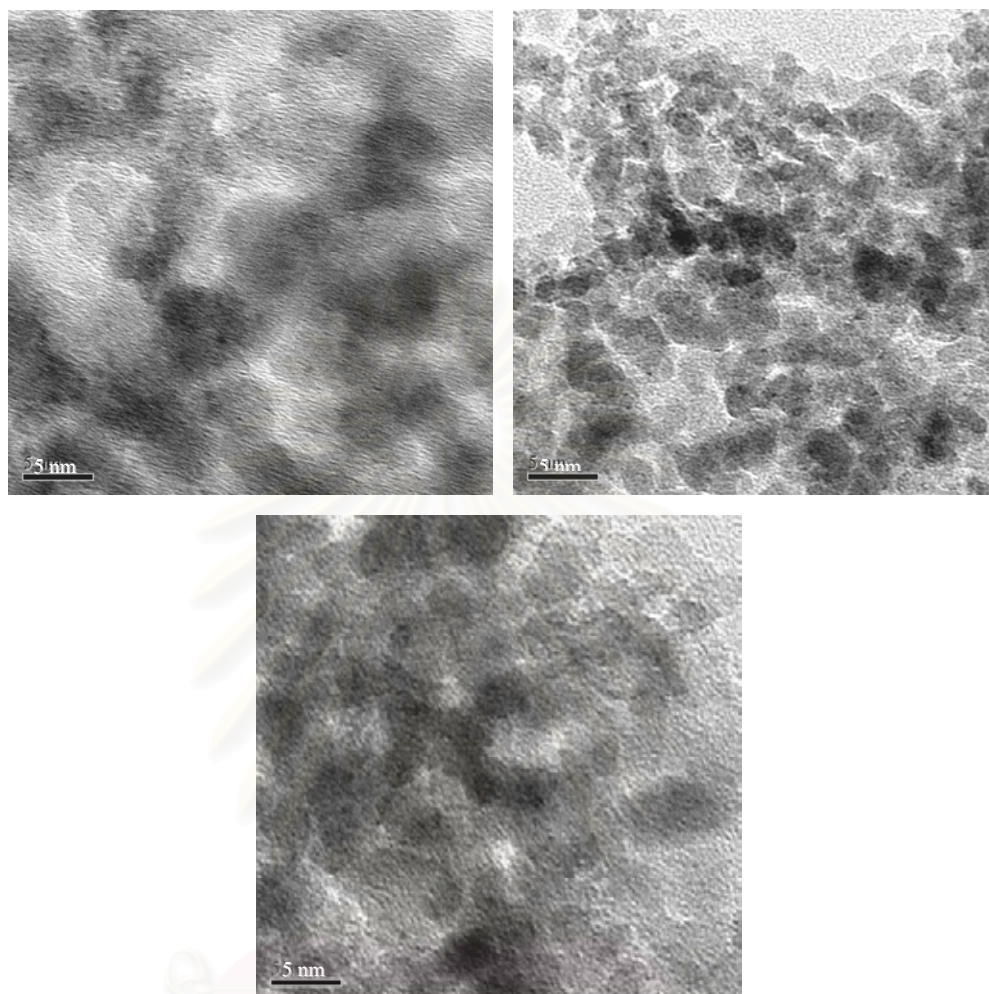
Figure 5.32   TEM micrographs of spent Pd/SiO$_2$-FSP with Pd loading 2 wt%
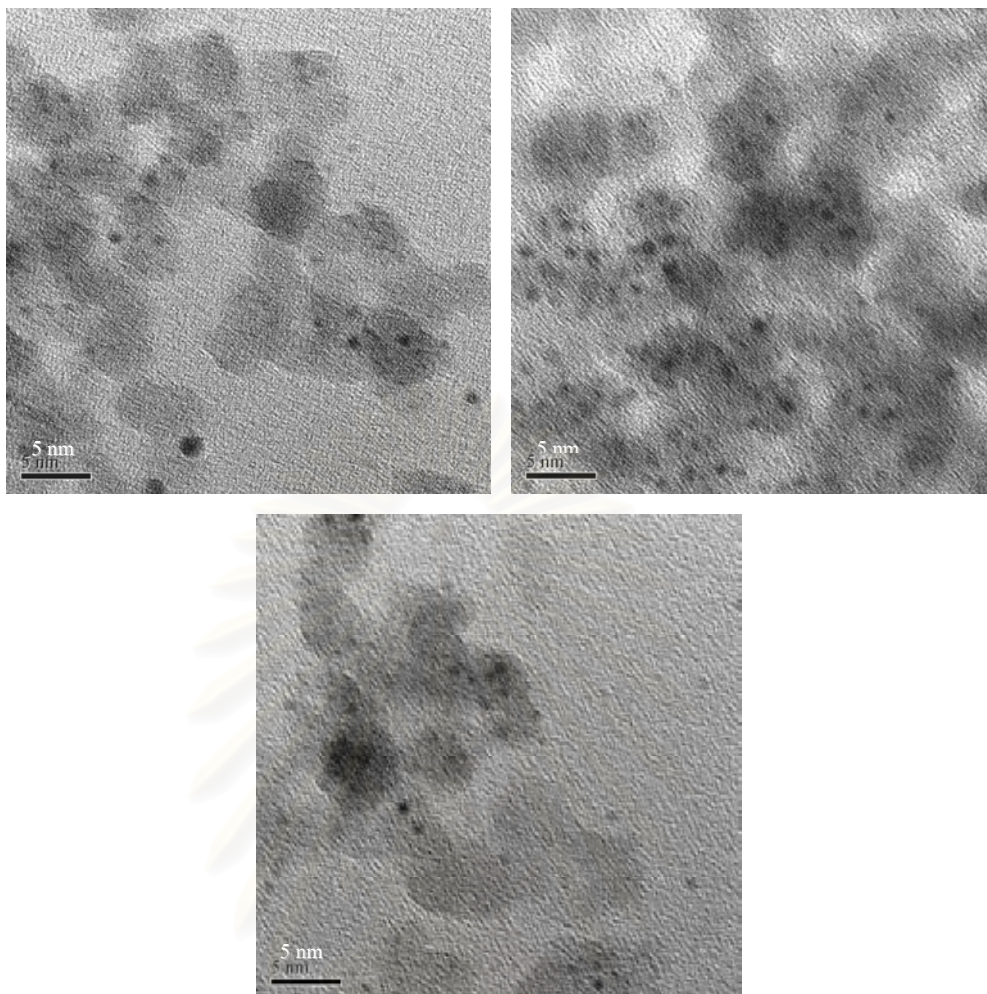
Figure 5.33   TEM micrographs of spent Pd/SiO$_2$-FSP with Pd loading 5 wt%
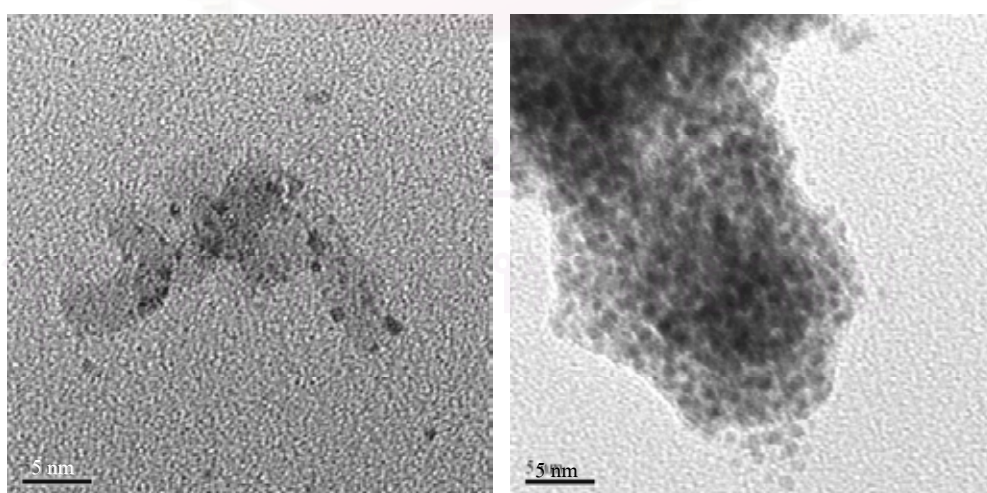
Figure 5.34   TEM micrographs of spent Pd/SiO2-FSP with Pd loading 10 wt%
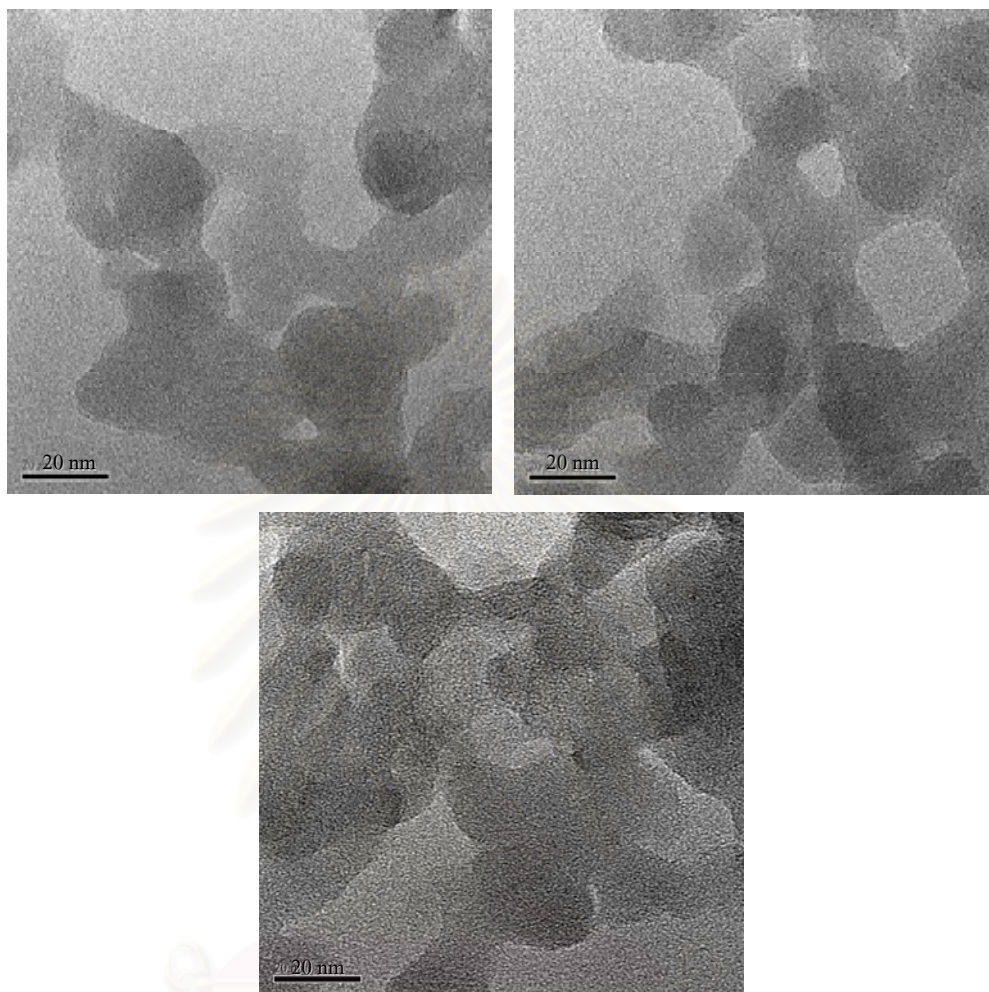
Figure 5.35 TEM micrographs of the impregnated-spent catalyst with Pd loading 0.5
wt%
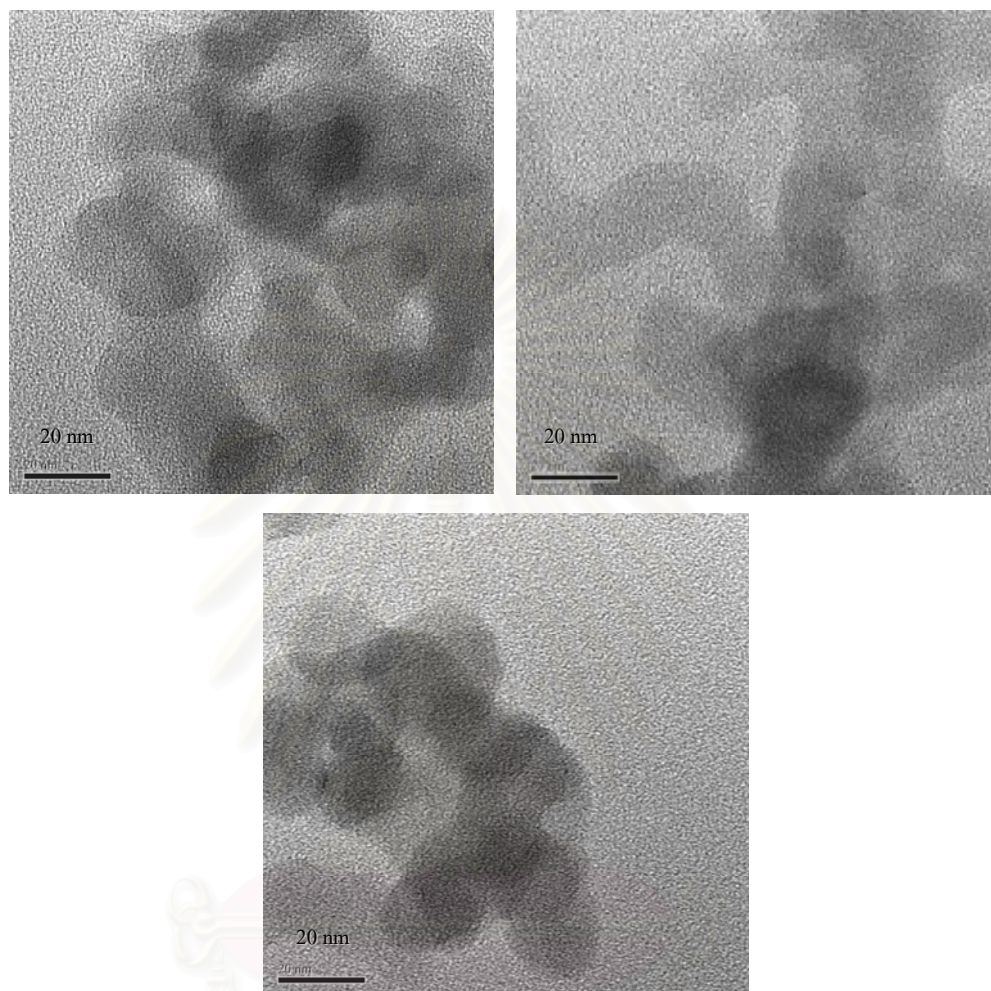
Figure 5. 36 TEM micrographs of the impregnated-spent catalyst with Pd loading 1
wt%
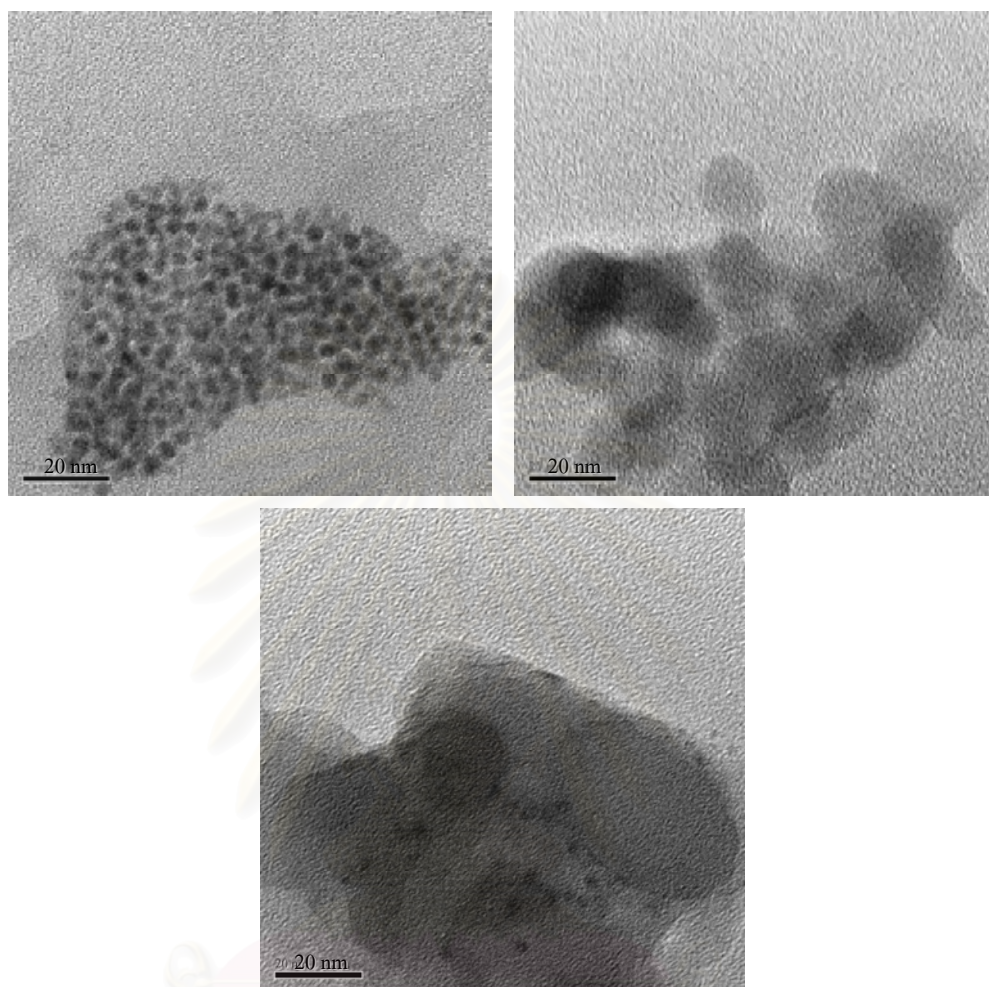
Figure 5. 37 TEM micrographs of the impregnated-spent catalyst with Pd loading 2 wt%
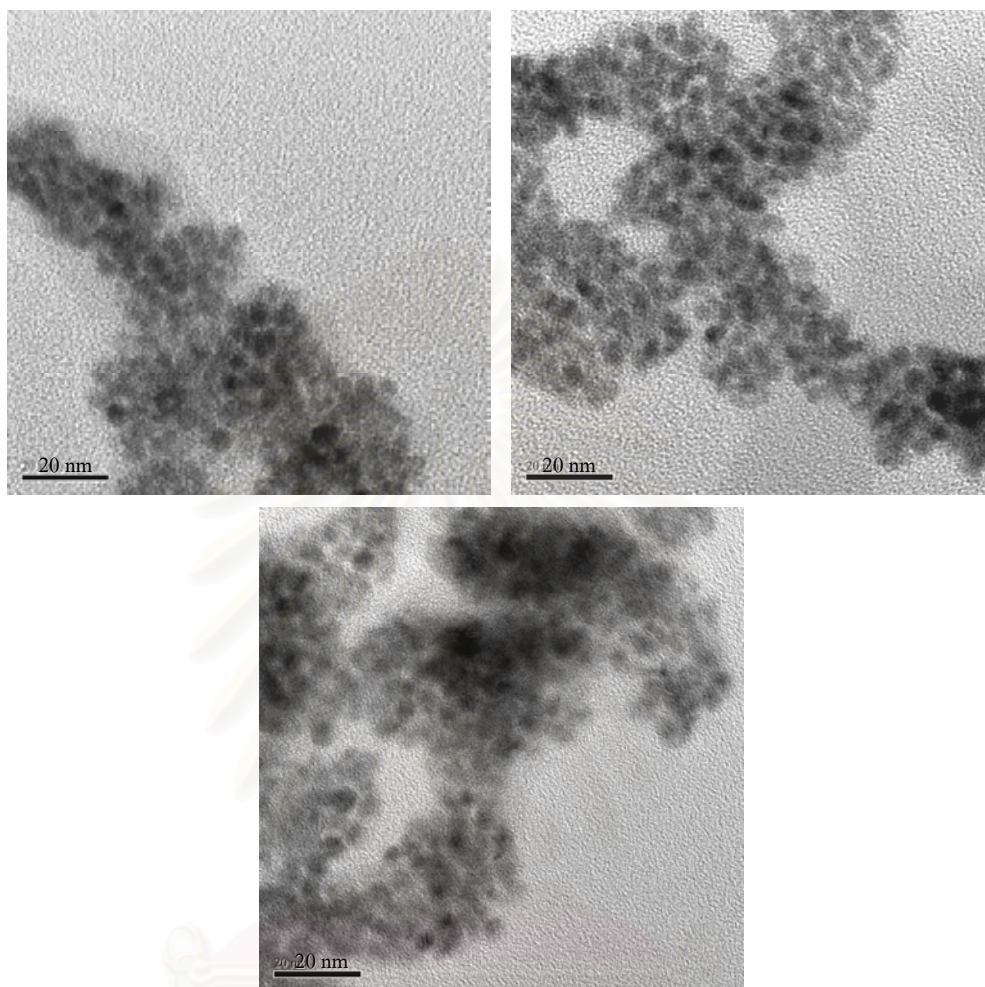
Figure 5.38 TEM micrographs of the impregnated-spent catalyst with Pd loading 5 wt%
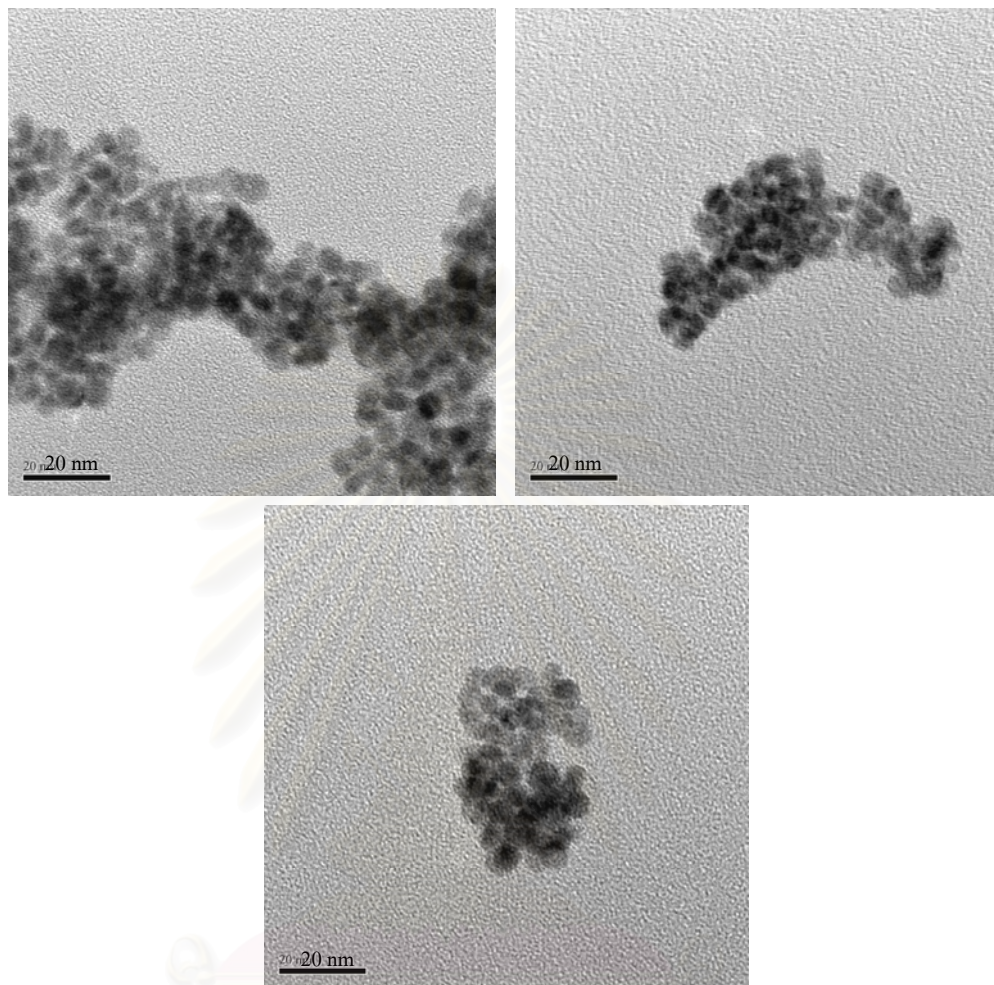
Figure 5.39   TEM micrographs of the impregnated-spent catalyst with Pd loading 10
wt%
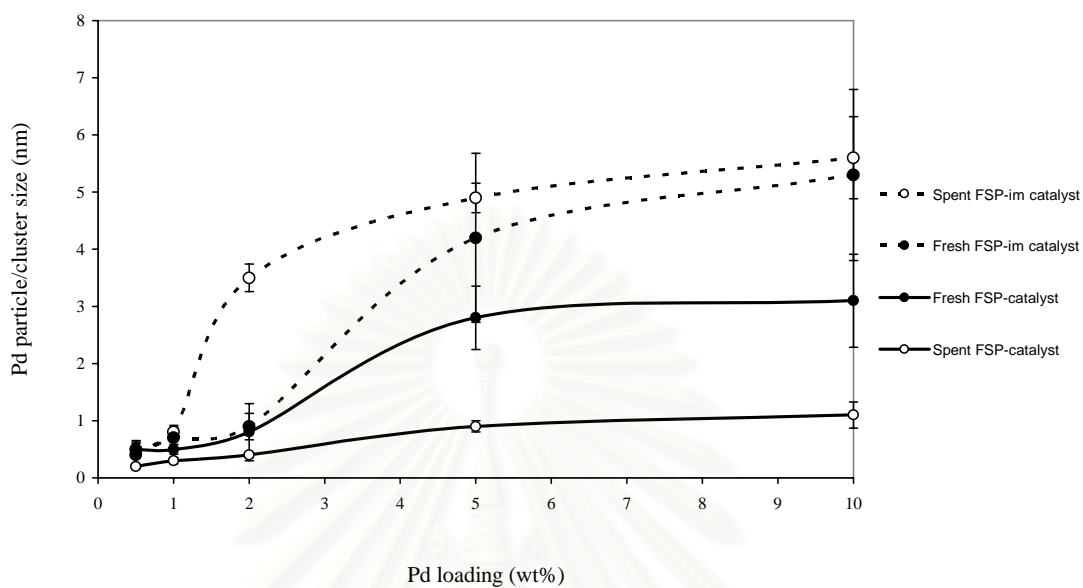
Figure 5.40 Plot between Pd size and Pd wt% loading (0.5 – 10 wt%) of fresh and
            spent catalysts of the flame-made and impregnated catalysts

For the flame-made 1 wt% Pd/SiO_2 catalyst and the 1 wt% Pd/SiO_2–com
catalyst, the catalytic activity decreased by 50 and 30% after the 3rd cycle of run,
respectively.

CHAPTER VI

CONCLUSIONS AND RECOMMENDATIONS

6.1 Conclusions

1. The flame spray pyrolysis method has been successfully applied for the one-step synthesis of Pd nanoparticles with average size of 0.5 to 3 nm on SiO_2 supports.

2. The as-synthesized one-step FSP-derived catalysts ($\leq$ 2 wt% Pd loading) showed higher catalytic activities in term of TOF for selective hydrogenation of 1-heptyne under mild conditions than the Pd impregnated on FSP-SiO_2 catalysts, Pd/SiO_2-com, and Lindlar catalyst. The remarkable high TOFs of the flame-made catalyst may be due to the strong Pd-Si interaction and/or the formation of Si-O groups covering the small Pd metal particles/clusters with resulted in CO suppression. However, there was no effect on the selectivities to 1-heptene.

3. Deactivation by metal sintering was found for Pd/SiO_2-FSP-im but not for Pd/SiO_2-FSP. However, catalytic activity decreased by 50 and 30% on the flame-made 1 wt% Pd/SiO_2 and 1 wt% Pd/SiO_2-com catalysts after the 3rd cycle of run, respectively.

6.2 Recommendation

1. The conditions for preparing catalysts by flame spray method should be adjusted such as the metal concentration, the feed flow rate etc.

2. Longer reaction time should be investigated in order to study the catalyst stability.

3. Causes for deactivation of Pd/SiO_2-FSP and Pd/SiO_2-FSP-im catalysts during liquid phase hydrogenation should be investigated.
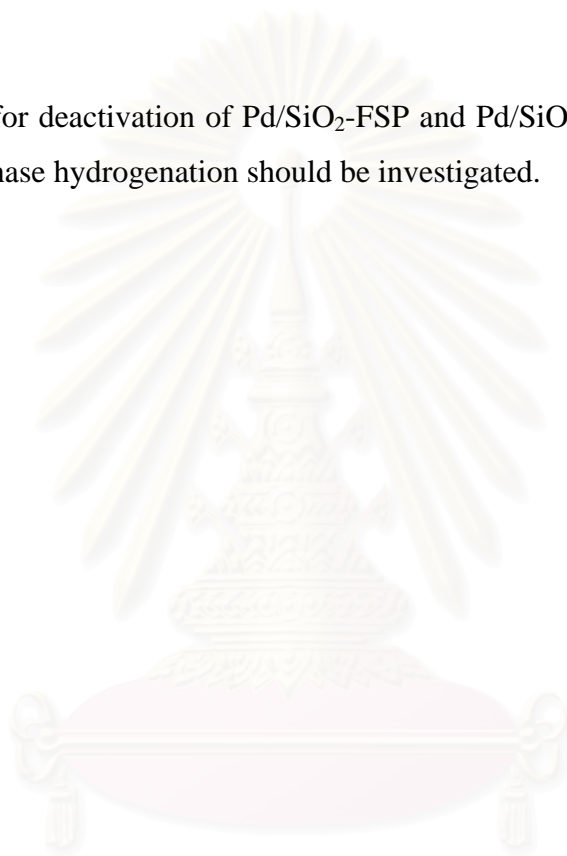
REFERENCES

[1]   A. Mastalir and Z. Kiraly Pd nanoparticles in hydrotalcite: mild and highly selective catalysts for alkyne semihydrogenation *J. Catal.* 202 (2003): 372-381.

[2]   R. Strobel, F. Krumeich, W.J. Stark, S.E. Pratsinis, and A. Baiker Flame spray synthesis of Pd/Al$_2$O$_3$ catalysts and their behavior in enantioselective hydrogenation *J. Catal.* 222 (2004): 307-314.

[3]   T.A. Nijhuis, G. van Koten, and J.A. Moulijin Optimized palladium catalyst systems for the selective liquid-phase hydrogenation of functionalyzed alkynes *App. Catal. A* 238 (2003): 259-271.

[4]   J. Panpranot, K. Phandinthong, P. Praserthdam, M. Hasegawa, S. Fujita, and M. Arai A comparative study of liquid-phase hydrogenation on Pd/SiO2 in organic solvents and under pressurized carbon dioxide: Activity change and metal leaching/sintering *J. Mol. Cat. A* 253 (2006): 20-24.

[5]   H. Blaser, A. Indolese, A. Schnyder, H. Steiner, and M. Studer Supported palladium catalysts for fine chemicals synthesis *J. Mol. Cat. A* 173 (2001): 3-18.

[6]   N. Marin-Astorga, G. Alvez-Manoli, and P. Reyes Stereoselective hydrogenation of phenyl alkyl acetylenes on pillared clays supported palladium catalysts *J. Mol. Cat. A* 226 (2005): 81-88.

[7]   A. Mastalir, Z. Kiraly, G. Szollosi, and M. Bartok Steroselctive hydrogenation of 1-phenyl-1-pentyne over low-loaded Pd-montmorillonite catalysts *App. Catal. A* 213 (2001): 133-140.

[8]   L. Hegedus and T. Mathe Selective heterogeneous catalytic hydrogenation of nitriles to promary amines in liquid phase Part I. Hydrogenation of benzonitrile over palladium *App. Catal. A* 296 (2005): 209-215.

[9]   E. Cagnola, D. Liprandi, M. Quiroga, and P. L'Argentiere 1-Heptyne semihydrogenation catalyzed by [PdCl$_2$(NH$_2$(CH$_2$)$_5$CH$_3$)$_2$] *React. Kinet. Catal. Lett.* 80 (2003): 277-283.

[10] H.D. Jang, H. Chang, Y. Suh, and K. Okuyama Synthesis of SiO$_2$ nanoparticles from sprayed droplets of tetraethylorthosilicate by the flame spray pyrolysis *Curr. App. Phys.* (2006).

[11] R. Strobel, W.J. Stark, L. Madler, S.E. Pratsinis, and A. Baiker Flame-made platinum/alumina: structural properties and catalytic behaviour in enantioselective hydrogenation *J. Catal.* 213 (2003): 296-304.

[12] J. Panpranot, O. Tangjitwattakorn, P. Praserthdam, J.G. Goodwin Jr. Effects of Pd precursors on the catalytic activity and deactivation of silica-supported Pd catalysts in liquid phase hydrogenation *App. Catal. A* 292 (2005): 322-327.

[13] L. Madler, H.K. Kammler, R. Mueller, and S.E. Pratsinis Controlled synthesis of nanostructured particles by flame spray pyrolysis *Aerosol Sci.* 33 (2002): 369-389.

[14] R. Mueller, Z. Madler, and S.E. Pratsinis Nanoparticles synthesis at high production rates by flame spray pyrolysis *Chem. Eng. Sci.* 58 (2003): 1969-1976.

[15] B. Marshall, I. Tefford, and R. Wood A field method for the determination of zinc oxide fume in air. *Analyst* 96 (1971): 569-578.

[16] M. Sokolowski, A. Sololowska, A. Michalski, and B. Gokieli The "in-flame-reaction" method for Al$_2$O$_3$ aerosol formation *J. Aerosol. Sci.* 8 (1977): 219-229.

[17] A.I.Y. Tok, F.Y.C. Boey, amd X.L. Zhao Novel synthesis of Al$_2$O$_3$ nano-particles by flame spray pyrolysis *J. Mater. Processing Technol.* (2006).

[18] C.R. Bickmore, K.F. Waldner, D.R. Treadwell, and R.M. Laine Ultrafine spinel powders by flame spray pyrolysis of a magnesium aluminum double alkoxide *J. Am. Ceram. Soc.* 79 (1996): 1419-1423.

[19] S. Grimm, M. Schultz, S. Barth, and R. Muller Flame pyrolysis – a preparation route for ultrafine pure γ–Fe$_2$O$_3$ powders and the control of their particle size and properties *J. Mater. Sci.* 32 (1997): 1083-1092.

[20] W.J. Stark, S.E. Pratsinis, and A. Baiker Flame made titania/silica epoxidation catalysts *J. Catal.* 203 (2001): 516-524.

[21] S. Hannemann, J. Grunwaldt, F. Krumeich, P. Kappen, A. Baiker, "Electron microscopy and EXAFS studies on oxid-supported gold-silver

nanoparticlas prepared by flame spray pyrolysis," *Applied Surface Science* 252 (2006) 7862-7873.

[22] S.D. Jackson and L.A. Shaw The liquid-phase hydrogenation of phenyl acetylene and styrene on a palladium/carbon catalyst *App. Catal. A* 134 (1996): 91-99.

[23] A. Molnar, A. Sarkany, and M. Varga Hydrogenation of carbon-carbon multiple bonds: chemo-, regio- and stereo-selectivity *J. Mol. Cat. A* 173 (2001): 185-221.

[24] P.C. L'Argentiere, E.A. Cagnola, M.E. Quiroga, and D.A. Liprandi A palladium tetra-coordinated complex as catalyst in the selective hydrogenation of 1-heptyne *App. Catal. A* 226 (2002): 253-263.

[25] M.G. Musolino, C.M.S. Cutrupi, A. Donato, D. Pietropaolo, and R. Pietropaolo Liquid phase hydrogenation of 2-butyne-1,4-diol and 2-butene-1,4-diol isomers over Pd catalysts: role of solvent, support and proton on activity and products distribution *J. Mol. Cat. A* 195 (2003): 147-157.

[26] A. Mastalir, Z. Kiraly, and F. Berger Comparative of size-quantized Pd-montmorillonite catalysts in liquid-phase semihydrogenations of alkynes *App. Catal. A* 269 (2004) 161-168.

[27] A. Papp, A. Molnar, and A. Masalir Catalytic investigation of Pd particles supported on MCM-41 for the selective hydrogenation of terminal and internal alkynes *App. Catal. A* 289 (2005): 256-266.

[28] P.A. Robles-Dutenhefner, M.G. Speziali, E.M.B. Sousa, E.N. Santos, and E.V. Gusevskaya Selective hydrogenation of myrcene catalyzed by sol-gel Pd/SiO$_2$ *App. Catal. A* 295 (2005): 52-58.

[29] P. Albers, J. Pietsch, and S.F. Parker Poisoning and deactivation of palladium catalysts *J. Mol. Cat. A* 173 (2001): 275-286.

[30] M. Besson and P. Gallezot Deactivation of metal catalysts in liquid phase organic reactions *Catal. Today* 81 (2003): 547-559.

[31] Kunnika Phandinthong, "Liquid-phase hydrogenation over palladium catalysts supported on sol-gel-derived silica," (Master's thiesis, Department of Chemical Engineering, Faculty of Engineering Chulalongkorn University, 2005)

[32] R. Strobel, F. Krumeich, W. J. Stark, S. E. Pratsinis, and A. Baiker Flame spray synthesis of Pd/Al$_2$O$_3$ catalysts and their behavior in enantioselective hydrogenation *J. Catal.* 200 (2004): 307-314.

[33] R. Stobel, W. J. Strak, L. Madler, S. E. Pratsinis, and A. Baiker Flame-made platinum/alumina: structure properties and catalytic behaviour in enantioselective hydrogenation *J. Catal.* 213 (2003): 296-304.

[34] T. Johannessen and S. Koutsopoulos One-step flame synthesis of an active Pt/TiO$_2$ catalyst for SO$_2$ oxidation – A possible alternative to traditional methods for parallel screening *J. Catal.* 205 (2002): 404-408.

[35] M. J. Height, S. E. Pratsinis, O. Mekasuwandumsong, and P. Praserthdam Ag-ZnO catalysts for UV-photodegradation of methylene blue *Appl. Catal. B* 63 (2006): 305.

[36] J. Panpranot, K. Phandinthong, P. Praserthdam, M. Hasegawa, S. Fujita, and M. Arai A comparative study of liquid-phase hydrogenation on Pd/SiO2 in organic solvents and under pressurized carbon dioside: Activity change and metal leaching/sintering *J. Mol. Cat. A* 253 (2006): 20-24.

[37] C. R. Lederhos, P. C. L'Argentiere, and N. S. Figoli 1-Heptyne selective hydrogenation over Pd supported catalysts *Ind. Eng. Chem. Res.* 44 (2005): 1752-1756.

[38] P.C. L'Argentiere, E.A. Cagnola, M.E. Quiroga, D.A. Liprandi A palladium tetra-coordinated complex as catalyst in the selective hydrogenation of 1-heptyne *App. Catal.* 226 (2002): 253-263.

[39] O. Dominguez-Quintero, S. Martineq, Y. Henriquez, L. D'Ornelas, H. Krentzien, J. Osuna Silica-supported palladium nanoparticles show remarkable hydrogenaion catalytic activity *J. Mol. Cat. A* 197 (2003): 185-191.

[40] X. Mu, U. Bartmann, M. Guraya, G.W. Busser, U. weckenmann, R. Fischer, M. Muhler The preparation of Pd/SiO$_2$ catalysts by chemical vapor deposition in a fluidized-bed reactor *App. Catal. A* 248 (2003): 85-95.

APPENDICES

APPENDIX A

CALCULATION FOR CATALYST PREPARATION

A.1 Flame Spray Pyrolysis Method

Preparation of 0 – 10 wt%Pd/SiO$_2$ catalysts by flame spray pyrolysis (FSP) are shown as follows:

Reagent: - Palldium acetylacetonate [Pd(acac)$_2$]

                    Molecular weight = 304.62 g

        - Tetraethylorthosilicate (TEOS)

                    Molecular weight = 208.33 g

                    Density = 0.934 g/ml

        - Acetonitrile

        - Xylene

Example calculation for the preparation of 0.5 wt%Pd/SiO$_2$-FSP

Based on 100 g for catalyst used, the composition of the catalyst will be as follows:

        Pd   = 0.5 g

        SiO$_2$ = 100 – 0.5   = 99.5 g

For 6 g of catalyst

        Pd required $= 6 \times \dfrac{0.5}{100}$ = 0.03 g

        SiO$_2$ required   = 6 – 0.03   = 5.97 g

Pd 0.03 g was prepared from Pd(acac)$_2$ and molecular weight of Pd is 106.4 as SiO$_2$ 5.97 g was prepared from TEOS and molecular weight of SiO$_2$ is 60.1

$$\text{Pd(acac)}_2 \text{ required} \quad = \frac{\text{MW of Pd(acac)}_2 \times \text{Pd required}}{\text{MW of Pd}}$$

$$= \frac{304.62 \times 0.03}{106.4} \quad = 0.0859 \text{ g}$$

$$\text{TOES required} \quad = \frac{\text{MW of TEOS} \times \text{SiO}_2 \text{ required}}{\text{MW of SiO}_2 \times \text{Density of TEOS}}$$

$$= \frac{208.33 \times 5.97}{60.1 \times 0.934} \quad = 22.3 \text{ ml}$$

Pd(acac)$_2$ and TEOS were dissolved in xylene/acetronitrile mixture (70/30 v/v). The total concentration of metal was always 0.5 M.

$$\text{mol of Pd required} \quad = \frac{0.03}{106.4} \quad = 2.82 \times 10^{-4} \text{ mol}$$

$$\text{mol of SiO}_2 \text{ required} \quad = \frac{5.97}{60.1} \quad = 0.099 \text{ mol}$$

$$\text{So,} \quad \text{volume of solution} \quad = \frac{(2.82 \times 10^{-4} + 0.099) \times 1000}{0.5} \quad = 200 \text{ ml}$$

For 200 ml of solution

$$\text{Solvent required} \quad = 200 - 22.3 \quad = 177.7 \text{ ml}$$

$$\text{Xylene required} \quad = \frac{70}{100} \times 177.7 \quad = 124.4 \text{ ml}$$

$$\text{Acetonitrile} \quad = 177.7 - 124.4 \quad = 53.3 \text{ ml}$$

A.2 Incipient Wetness Impregnation Method

Preparation of 0.5 – 10 wt%Pd/SiO$_2$ catalysts by impregnation method are shown as follows:

Reagent: - Palldium acetylacetonate [Pd(acac)$_2$]

Molecular weight = 304.62 g

- Support: SiO$_2$ prepared by flame spray pyrolysis

- Acetonitrile

Example calculation for the preparation of 0.5 wt%Pd/SiO$_2$-imp-FSP

Based on 100 g for catalyst used, the composition of the catalyst will be as follows:

Pd   = 0.5 g

SiO$_2$ = 100 – 0.5   = 99.5 g

For 0.5 g of catalyst

Pd required $= 0.5 \times \dfrac{0.5}{100}$ = 0.0025 g

SiO$_2$ required   = 0.5 – 0.0025   = 0.4975 g

Pd 0.0025 g was prepared from Pd(acac)$_2$ and molecular weight of Pd is 106.4.

Pd(acac)$_2$ required $= \dfrac{\text{MW of Pd(acac)}_2 \times \text{Pd required}}{\text{MW of Pd}}$

$= \dfrac{304.62 \times 0.0025}{106.4}$ = 0.0072 g

APPENDIX B

CALCULATION FOR METAL ACTIVE SITES AND DISPERSION

Calculation of the metal active sites and metal dispersion of the catalyst, a stoichiometry of CO/Pd = 1, measured by CO adsorption is as follows:

Let the weight of catalyst used	=	W	g
Integral area of CO peak after adsorption	=	A	unit
Integral area of 75 μl of standard CO peak	=	B	unit
Amounts of CO adsorbed on catalyst	=	B-A	unit

Volume of CO adsorbed on catalyst $\quad = \quad 75 \times \dfrac{(B-A)}{B} \quad$ μl

Volume of 1 mole of CO at 30°C $\quad = \quad 24.86 \times 10^6 \quad$ μl

Mole of CO adsorbed on catalyst $\quad = \quad \dfrac{75}{24.86 \times 10^6} \times \dfrac{(B-A)}{B} \quad$ μmole

Molecule of CO adsorbed on catalyst $= [1.61 \times 10^{-6}] \times [6.02 \times 10^{23}] \times \dfrac{(B-A)}{B}$ molecules

Metal active sites $\quad = \quad [9.68 \times 10^{17}] \times \dfrac{(B-A)}{B} \times \dfrac{1}{W} \quad$ molecules of CO/g of catalyst

Molecules of Pd loaded $\quad = \quad [6.02 \times 10^{23}] \times \dfrac{[\%wt\ of\ Pd]}{[MW\ of\ Pd]}$ molecules/g of catalyst

Metal dispersion (%) $\quad = \quad 100 \times \dfrac{\text{moleculed of Pd from CO adsorption}}{\text{molecules of Pd loaded}}$

APPENDIX C

CALIBRATION CURVES

This appendix showed the calibration curve for calculation of composition of reactant and products in 1-heptyne hydrogenation. The reactant is 1- heptyne and products are 1-heptene and n-heptane.

The flame ionization detector (FID), gas chromatography Shimadzu modal 14B was used for analyzing the concentration of 1-heptyne, 1-heptene and n-heptane by using GS-alumina column.

The GS-alumina column was used with a gas chromatography equipped with a flame ionization detector (FID), Shimadzu modal 14B, for analyzing the concentration of 1-heptyne, 1-heptene and n-heptane. Condition uses in GC are illustrated in Table C.1.

Mole of reagent in y-axis and area, which was reported by gas chromatography, in x-axis is exhibited in the curves. The calibration curves of 1-heptyne and 1-heptene.

Table C.1   Conditions uses in Shimadzu modal GC-14B

Parameters	Conditions of Shimadzu GC-14B
Width	5
Slope	29
Drift	0
Min. area	20
T. DBL	2.7
Stop time	10
Atten.	0
Speed	2
Method	1
Format	1
SPL. WT	100
IS. WT	0
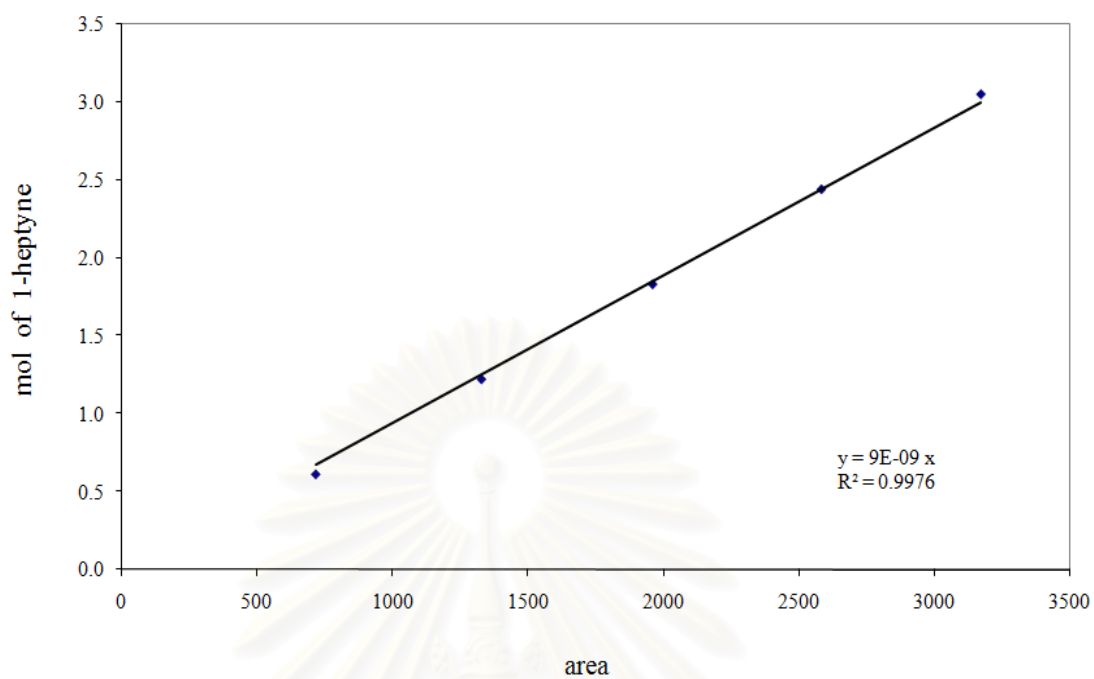
Figure C.1   The calibration curve of 1-heptyne
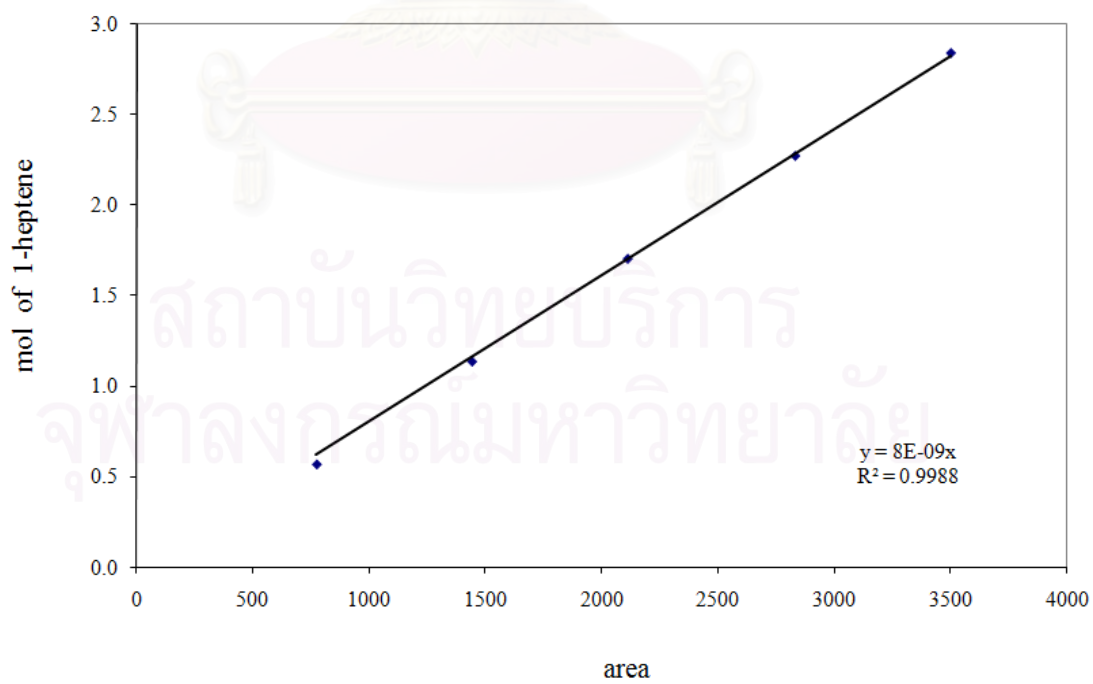
Figure C.2 The calibration curve of 1-heptene

APPENDIX D

CALCULATION OF 1-HEPTYNE CONVERSION
AND 1-HEPTENE SELECTIVITY

The catalytic performance for the 1-heptyne hydrogenation was evaluated in terms of activity for 1-heptyne conversion and 1-heptene selectivity.

Activity of the catalyst performed in term of 1-heptyne conversion. 1-Heptyne conversion is defined as moles of 1-heptyne converted with respect to 1-heptyne in feed:

$$\text{1-heptyne conversion (\%)} \quad = \quad 100 \times \frac{\text{mole of 1- heptyne in (feed - product)}}{\text{mole of 1- heptyne in feed}} \quad \text{(D.1)}$$

Where mole of 1-heptyne can be measured employing the calibration curve of 1-heptyne in Figure C.1, Appendix C.

$$\text{Mole of 1-heptyne} \quad = \quad \left(\begin{array}{c} \text{Area of 1- heptyne peak} \\ \text{from integrator plot on GC -14B} \end{array} \right) \times (9 \times 10^{-9}) \quad \text{(D.2)}$$

Selectivity of product is defined as mole of 1-heptene formed with respect to mole of 1-heptyne converted:

$$\text{1-heptene selectivity (\%)} \quad = \quad 100 \times \frac{\text{mole of 1- heptene formed}}{\text{mole of total product}} \quad \text{(D.3)}$$

Where mole of 1-heptene can be measured employing the calibration curve of 1-heptene in Figure C.2, Appendix C.

$$\text{Mole of 1-heptene} = \left(\frac{\text{Area of 1-heptene peak}}{\text{from integrator plot on GC-14B}} \right) \times (8 \times 10^{-9}) \qquad \text{(D.2)}$$

APPENDIX E

CALCULATION OF TURNOVER OF FREQUENCY

Metal active site $\quad = \quad y \quad$ molecule/g catalysts

$$TOF \quad = \quad \frac{rate}{(number\ of\ active\ site)}$$

$$= \quad \frac{[molecule\ substrate\ conveted]}{[g\ cat.][min]} \left| \frac{[g\ cat.]}{y\ [active\ site]} \right| \frac{[min]}{[s]}$$

$$= \quad [s^{-1}]$$

APPENDIX F

LIST OF PUBLICATION

1. Sirima Somboonthanakij, Joongjai Panpranot, and Okorn Mekasuwandumrong. Liquid-phase semihydrogenation of 1-heptyne over nano-Pd/SiO$_2$ catalysts prepared by flame spray pyrolysis. *Proceedings of the Regional Symposium on Chemical Engineering 2006*, Singapore, Dec 3 – 5, 2006.

2. Sirima Somboonthanakij, Okorn Mekasuwandumrong, Joongjai Panpranot, Tarit Nimmanwudtipong, Reto Strobel, Sotiris E. Pratsinis, and Piyasan Praserthdam. Characteristics and catalytic properties of Pd/SiO$_2$ synthesized by one-step flame spray pyrolysis in liquid-phase hydrogenation of 1-heptyne. *Catalysis Letters* (2007), in press.

VITA

Miss Sirima Somboonthanakij was born in July 4th, 1983 in Bangkok, Thailand. She finished high school from Saipanya School, Bangkok in 2001, and received bachelor's degree in the department of Chemical Science from Faculty of Science, Chulalongkorn University, Bangkok, Thailand in 2005.